USGS
science for a changing world

Prepared in cooperation with the Bureau of Reclamation

Hydrogeologic Characterization of the Hualapai Plateau on the Western Hualapai Indian Reservation, Northwestern Arizona

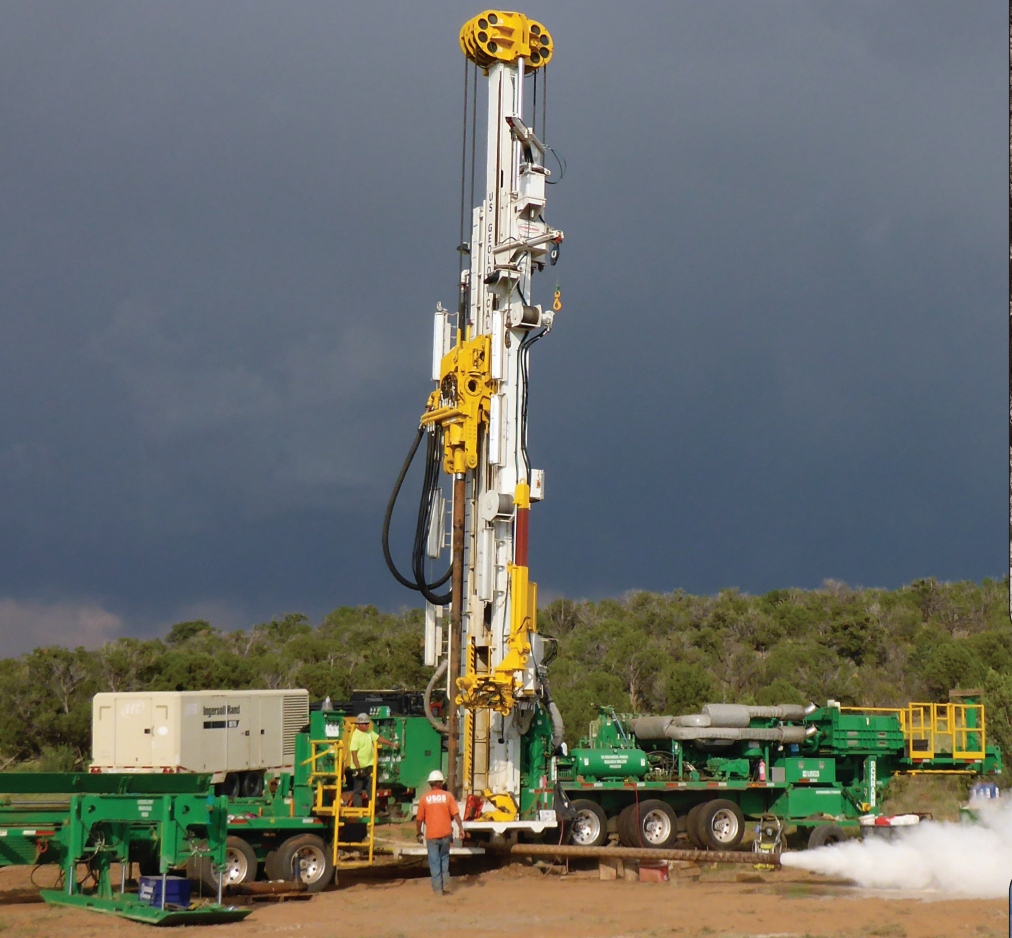

Scientific Investigations Report 2020–5025

U.S. Department of the Interior
U.S. Geological Survey

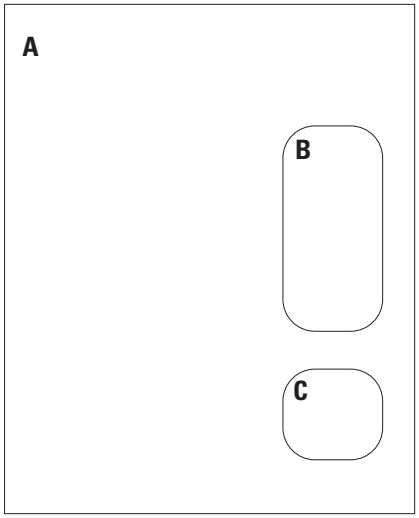

Cover A. U.S. Geological Survey photograph of the Hualapai Test Well being drilled in 2018 on Horse Flat. Photograph by Jon Mason, August 2018.

Cover B. U.S. Geological Survey photograph of Travertine Falls in Travertine Canyon. This site is the location of a spring referred herein as the Travertine Canyon above the mouth. Photograph by Casey Jones, May 2018.

Cover C. Aerial photograph of the northern Hualapai Plateau taken between Horse Flat and Quartermaster Canyons, looking south. U.S. Geological Survey photograph taken by Jon Mason, July 2016

Hydrogeologic Characterization of the Hualapai Plateau on the Western Hualapai Indian Reservation, Northwestern Arizona

By Jon P. Mason, Jamie P. Macy, Donald J. Bills, Bruce W. Gungle, and Casey J. Jones

Prepared in cooperation with the Bureau of Reclamation

Scientific Investigations Report 2020–5025

U.S. Department of the Interior
U.S. Geological Survey

U.S. Department of the Interior
DAVID BERNHARDT, Secretary

U.S. Geological Survey
James F. Reilly II, Director

U.S. Geological Survey, Reston, Virginia: 2020

Suggested citation:
Mason, J.P., Macy, J.P., Bills, D.J., Gungle, B.W., and Jones, C.J., 2020, Hydrogeologic characterization of the Hualapai Plateau on the western Hualapai Indian Reservation, northwestern Arizona: U.S. Geological Survey Scientific Investigations Report 2020–5025, 38 p, https://doi.org/10.3133/sir20205025.

Associated data for this publication:
Macy, J.P., 2019, Controlled source audio-frequency magnetotellurics (CSAMT) data from the Grand Canyon West and Plain Tank Flat areas of the western Hualapai Reservation, Arizona: U.S. Geological Survey data release, https://doi.org/10.5066/P90KAJM4.

ISSN 2328-0328 (online)

Contents

Figures

Tables

Conversion Factors

U.S. customary units to International System of Units

Multiply	By	To obtain
	Length	
inch (in.)	2.54	centimeter (cm)
inch (in.)	25.4	millimeter (mm)
foot (ft)	0.3048	meter (m)
mile (mi)	1.609	kilometer (km)
yard (yd)	0.9144	meter (m)
	Area	
Acre	4,047	square meter (m^2)
Acre	0.4047	hectare (ha)
Acre	0.4047	square hectometer (hm^2)
Acre	0.004047	square kilometer (km^2)
square foot (ft^2)	0.09290	square meter (m^2)
section (640 acres or 1 square mile)	259.0	square hectometer (hm^2)
square mile (mi^2)	259.0	hectare (ha)
square mile (mi^2)	2.590	square kilometer (km^2)
	Volume	
gallon (gal)	3.785	liter (L)
gallon (gal)	0.003785	cubic meter (m^3)
cubic foot (ft^3)	0.02832	cubic meter (m^3)
acre-foot (acre-ft)	1,233	cubic meter (m^3)
acre-foot (acre-ft)	0.001233	cubic hectometer (hm^3)
	Flow rate	
acre-foot per day (acre-ft/d)	0.01427	cubic meter per second (m^3/s)
acre-foot per year (acre-ft/yr)	1,233	cubic meter per year (m^3/yr)
acre-foot per year (acre-ft/yr)	0.001233	cubic hectometer per year (hm^3/yr)
foot per second (ft/s)	0.3048	meter per second (m/s)
foot per minute (ft/min)	0.3048	meter per minute (m/min)
foot per day (ft/d)	0.3048	meter per day (m/d)
foot per year (ft/yr)	0.3048	meter per year (m/yr)
cubic foot per second (ft^3/s)	0.02832	cubic meter per second (m^3/s)
cubic foot per day (ft^3/d)	0.02832	cubic meter per day (m^3/d)
gallon per minute (gal/min)	0.06309	liter per second (L/s)

Multiply	By	To obtain
	Flow rate —Continued	
gallon per day (gal/d)	0.003785	cubic meter per day (m^3/d)
	Mass	
pound, avoirdupois (lb)	0.4536	kilogram (kg)
	Pressure	
inch of mercury at 60 °F (in Hg)	3.377	kilopascal (kPa)
	Radioactivity	
picocurie per liter (pCi/L)	0.037	becquerel per liter (Bq/L)
	Specific capacity	
gallon per minute per foot ([gal/min]/ft)	0.2070	liter per second per meter ([L/s]/m)
	Hydraulic conductivity	
foot per day (ft/d)	0.3048	meter per day (m/d)
	Hydraulic gradient	
foot per mile (ft/mi)	0.1894	meter per kilometer (m/km)
	Transmissivity	
foot squared per day (ft^2/d)	0.09290	meter squared per day (m^2/d)

Temperature in degrees Celsius (°C) may be converted to degrees Fahrenheit (°F) as follows:

$$°F = (1.8 \times °C) + 32.$$

Temperature in degrees Fahrenheit (°F) may be converted to degrees Celsius (°C) as follows:

$$°C = (°F - 32) / 1.8.$$

Datum

Vertical coordinate information is referenced to the National Geodetic Vertical Datum of 1929 (NGVD 29) and North American Vertical Datum of 1988 (NAVD 88).

Horizontal coordinate information is referenced to the North American Datum of 1983 (NAD 83).

Altitude, as used in this report, refers to distance above the vertical datum.

Supplemental Information

Specific conductance is given in microsiemens per centimeter at 25 degrees Celsius (µS/cm at 25 °C).

Concentrations of chemical constituents in water are given in either milligrams per liter (mg/L) or micrograms per liter (µg/L).

Activities for radioactive constituents in water are given in picocuries per liter (pCi/L).

Results for measurements of stable isotopes of an element (with symbol E) in water, solids, and dissolved constituents commonly are expressed as the relative difference in the ratio of the number of the less abundant isotope (iE) to the number of the more abundant isotope of a sample with respect to a measurement standard.

Abbreviations

BCM	Basin Characterization Model
BIA	Bureau of Indian Affairs
CSAMT	controlled source audio-frequency magnetotellurics
D	depth of investigation
DOI	Department of the Interior
ET	evapotranspiration
E_x	parallel electrical-field strength
E_y	perpendicular electrical-field strength
f	frequency
H_x	parallel magnetic-field strength
HDNR	Hualapai Department of Natural Resources
H_y	perpendicular magnetic-field strength
H_z	vertical magnetic-field strength
MT	magnetotelluric
NRCE	Natural Resources Consulting Engineers
PRISM	Parameter-Elevation Relationships on Independent Slopes Model
r	separation between the transmitter and receiver
USGS	U.S. Geological Survey
ρ_a	apparent resistivity

Hydrogeologic Characterization of the Hualapai Plateau on the Western Hualapai Indian Reservation, Northwestern Arizona

By Jon P. Mason, Jamie P. Macy, Donald J. Bills, Bruce W. Gungle, and Casey J. Jones

Abstract

This study was developed to assess if groundwater from the western Hualapai Plateau could be used to supply developments in the Grand Canyon West area of the Hualapai Indian Reservation and to collect hydrogeologic data for future use in a numerical groundwater model for the reservation. Ground-based geophysical surveys; existing well, spring, and other hydrogeologic information from previous studies; and new well and spring data collected for this study were used to provide a better understanding of the hydrogeology of the western Hualapai Plateau.

Surface geophysical data provided information on the depth and geologic structure of lower Paleozoic rock units and Proterozoic crystalline and metamorphic rocks that underlie the western Hualapai Plateau. The surface geophysical data and discharge information from springs were used to select a site to drill and develop the U.S. Geological Survey Hualapai Test Well.

The Hualapai Test Well was drilled to understand the geophysical properties of geologic formations at depth. These data were used to verify the results of surface geophysical data and to evaluate if sufficient water was present in the Hualapai Test Well for potential groundwater development. The Hualapai Test Well was drilled to a depth of 2,468 feet and bottomed in Proterozoic granite. Water was expected in the lower part of the Muav Limestone, but water was not observed until the Tapeats Sandstone at a depth of 2,400 feet. The Tapeats Sandstone was determined to be confined with a hydrostatic head of over 900 feet. A 48-hour pumping test was conducted to determine aquifer properties. Low specific capacity indicated that although groundwater is present in the Tapeats Sandstone, well yields are likely to be small. A water-quality sample indicated the sample had a calcium, magnesium-bicarbonate water type with a total dissolved-solids concentration of 371 milligrams per liter. Alpha radioactivity of the sample, 18.3 picocuries per liter, exceeded the U.S. Environmental Protection Agency maximum contaminant level of 15 picocuries per liter for drinking water. Concentrations of iron and manganese in the water sample also exceeded the U.S. Environmental Protection Agency secondary maximum contaminant levels for drinking water.

An inventory of wells and springs provided insight into the occurrence of groundwater on the western Hualapai Plateau. Data from 56 springs on and adjacent to the western Hualapai Plateau were compiled for this study, and new data were collected at 31 springs. Discharge from springs visited for this study ranged from dry to about 345 gallons per minute. The temporal data from springs, where repeat measurements were available, indicated that spring flow is highly variable and likely related to seasonal and annual precipitation. Water levels from 36 wells on and adjacent to the western Hualapai Plateau were compiled for this study, and new water levels were collected at 5 wells. The spring and well data in conjunction with the Hualapai Test Well results indicated that on the western Hualapai Plateau, bedrock aquifers have limited discrete flow paths that make extensive groundwater development unlikely.

Introduction

The primary regional aquifer on the western Hualapai Plateau is the Muav Limestone aquifer, hereafter called the Muav aquifer, which is composed of the Cambrian Muav Limestone. In other areas of the Colorado Plateau, the Muav Limestone is considered part of the Redwall-Muav aquifer system. However, the results from this study and observations made by previous studies such as Twenter (1962) indicate that the Redwall Limestone is unsaturated on the western Hualapai Plateau. For this reason, the term Muav aquifer, instead of Redwall-Muav aquifer, is used in this report. The confined to unconfined Muav aquifer supports groundwater discharge to springs at the western end of the Grand Canyon on the Hualapai Plateau and along the Grand Wash Cliffs both on and off reservation lands. Groundwater use from this aquifer was minor throughout the 20th century, consisting mostly of small community public supply, domestic, and agricultural uses (Bills and others, 2007; Arizona Department of Water Resources, 2009). The westernmost part of the Muav aquifer underlies the western Hualapai Plateau and is a largely undeveloped source of water for the Hualapai Tribe (fig. 1). Spring discharge from the aquifer has been a water supply for livestock and wildlife resources both on and off reservation lands since before the 1883 designation of the Hualapai

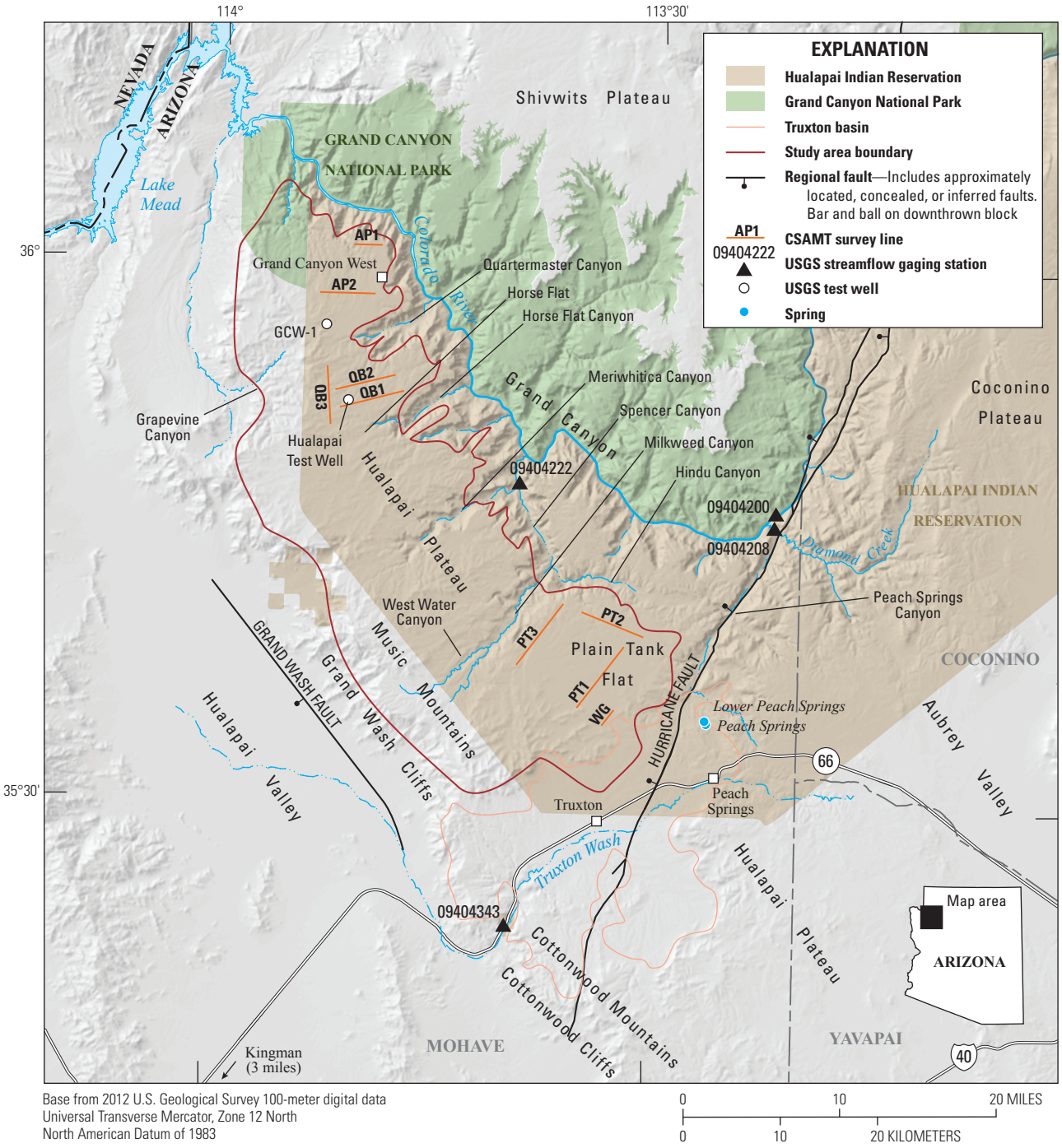

Figure 1. Map of the western Hualapai Indian Reservation and adjacent areas in northwestern Arizona showing physiographic features and study area boundary. Faults modified from Arizona Bureau of Geology and Mineral Technology (1988), Beard and Lucchitta (1993), Richard and others (2000), and Billingsley and others (2006).

Indian Reservation. Most of the groundwater discharge from the Muav aquifer occurs as spring flow in tributaries to the Colorado River above Lake Mead.

The Grand Canyon West Development (fig. 1), an important economic resource for the Hualapai Tribe at the northern end of the western Hualapai Plateau (Hualapai Department of Natural Resources, 2010), currently receives its water by a pipeline from wells and springs in Tertiary rock units 27 miles (mi) to the south in West Water Canyon (Stantec, 2009). Given the future water needs projected by the Hualapai Tribe development project, a concern is the groundwater resources contained in the Tertiary rocks and gravels on the western Hualapai Plateau might not remain a sustainable source of water (Hualapai Department of Natural Resources, 2010; Stantec, 2009).

The physical characteristics of the Muav aquifer vary laterally and with depth across northern Arizona. The depth, thickness, and geologic structure of the Muav Limestone determine where the Muav aquifer contains significant groundwater flow. The Hualapai Indian Reservation is nearly

divided in half by the northeast-southwest trending Hurricane Fault, which also forms part of the eastern boundary of the study area. How this fault affects groundwater flow is unknown, but faults are often barriers or conduits of flow. Paleozoic and Tertiary rocks are dominant throughout the western Hualapai Plateau, which is bisected by a series of mainly northeast flowing, deeply incised tributary drainages to the Colorado River (fig. 1).

The groundwater-storage capacity of the western Hualapai Plateau is unknown, and the occurrence and movement of groundwater is inferred only by the location and discharge of springs. Regional groundwater flow is assumed to be from the southwest to northeast, on the basis of regional dip of the rocks and the abundance of springs in the Grand Canyon and lack of them in the Grand Wash Cliffs. Only one well, GCW-1, located a few miles to the southwest of the Grand Canyon West Development, was drilled and developed in Paleozoic rocks on this part of the reservation. At the location of the well, the Redwall and Muav Limestones were dry, and groundwater was not encountered until penetration of the Tapeats Sandstone (2,660 ft below land surface). The well was only marginally successful with a yield of 15 to 25 gallons per minute (gal/min). Watt (Bureau of Reclamation; written commun., 2000) reported water quality was generally good but exceeded the U.S. Environmental Protection Agency (EPA) primary drinking water standards for coliform bacteria, arsenic, gross alpha, and combined radium.

In 2016, as a part of ongoing studies of groundwater resources on the Hualapai Plateau, the Bureau of Reclamation requested that the U.S. Geological Survey (USGS) update information on, and evaluate the groundwater resources of, the western Hualapai Plateau. This study was meant to identify a potential long-term source of water supply for the Grand Canyon West area. The Muav aquifer was thought to be the most likely local source of new groundwater in the western part of the reservation. The study was developed to provide an understanding of aquifer properties where it underlies the western part of the reservation. Surface geophysical methods were used to develop a better understanding of aquifer characteristics, such as depth, thickness, and geologic structure, on the western Hualapai Plateau. Additionally, an inventory of wells and springs provided insight into the occurrence of groundwater on the western Hualapai Plateau, and a new test well, the Hualapai Test Well, provided valuable hydraulic information about bedrock aquifers in this area.

Purpose and Scope

This report describes the collection and evaluation of surface geophysical data, the lithology and logging data obtained from the construction of the Hualapai Test Well (appendix 1; Macy, 2019), data collected from an inventory of wells and springs (appendix 2; U.S. Geological Survey, 2019), a compilation of existing lithologic data from borehole logs, precipitation and recharge estimates, water use, and water-level data. These data were used to improve knowledge of Muav aquifer characteristics and to determine the depth to the impermeable crystalline and metamorphic bedrock basement. The occurrence and extent of perched water-bearing zones are also discussed in relation to the regional Muav aquifer.

Previous Investigations

The Hualapai Indian Reservation was established in 1883 with the northern boundary defined by the Colorado River (fig. 1). Early work on the geology of the Hualapai Indian Reservation was conducted as reconnaissance by several USGS geologists including Dutton (1882a, b), Lee (1908), Schrader (1909), Darton (1910, 1915, 1925), and McKee (1934, 1938, 1945). Other early researchers who worked in this area include Koons (1945; 1948a, b), who described the geology of the Hualapai Indian Reservation proceeding westward from the eastern Grand Canyon. The Arizona Geological Survey produced a geologic map of Mohave County, including Hualapai Indian Reservation lands in 1959, and a geologic map of Arizona in 1969, which have been revised several times since (Wilson and Moore, 1959; Reynolds, 1997; Richards and others, 2000).

In cooperation with the Bureau of Indian Affairs (BIA), the USGS evaluated the geology and hydrology of the Hualapai Indian Reservation (Twenter, 1962). The basin-fill sediments and Muav Limestone of the Truxton basin were identified as potential sources of groundwater resources for the Hualapai Indian Reservation. Researchers outside of the USGS, such as Boyer (1977) and Boyer and others (1978), made recommendations for water management and development based on an inventory of stock ponds on the reservation, discharge measurements of large springs, and evaluation of selected wells. Boyer (1977) also recommended the collection of detailed geophysical information to better understand local groundwater supply. Huntoon (1977, 1978) and Young (1978) discussed Cambrian stratigraphic nomenclature and difficulties with groundwater development on the Hualapai Plateau.

Throughout the 1970s and 1980s, the Arizona Department of Water Resources and the USGS cooperated on a series of groundwater elevation maps for areas in Arizona including the Peach Springs Basin (Myers, 1987), which includes the Hualapai Plateau. They determined that most of the spring discharge on the western Hualapai Indian Reservation comes from either aquifers made of basin-fill sediment or the Muav aquifer, although most large springs discharge from the Muav aquifer. A series of four 1:48,000-scale geologic maps focused on mineral resource potential improved the detail and understanding of the surface geology and geologic structure on reservation lands (Billingsley and others, 1986, 1999; Wenrich and others, 1996, 1997; Billingsley and others, 2006).

In 1994, the USGS began to collect streamflow data, in cooperation with the Hualapai Tribe, at three streamflow-gaging stations: Truxton Wash near Valentine, Ariz. (09404343); Spencer creek, an informally named perennial stream within Spencer Canyon, near Peach Springs, Ariz. (09404222); and

Diamond Creek near Peach Springs, Ariz. (09404208) (fig. 1). Flow-rate and water-quality data have been collected for most of the springs and selected wells on the reservation (Hualapai Water Resources Program, 1999, 2004, 2009).

Access to sustainable quantities of good-quality water has been a goal of the Hualapai Tribe for decades. Young (2007) described perched groundwater resources contained in the river gravels and semiconsolidated sediments of the West Water Canyon area that have since been developed as a source of water for the growing Grand Canyon West Development. Watt (Bureau of Reclamation; written commun., 2000) and Natural Resources Consulting Engineers (2011) described the lithology and water resources observed in the single bedrock well (GCW-1) drilled in the Grand Canyon West area.

Description of Study Area

The study area is defined here as the western part of the Hualapai Plateau that extends northwest from the Truxton basin to north of Grand Canyon West, west to the Grand Wash Cliffs, and north towards the Colorado River (Trapp and Reynolds, 1995; fig. 1). The study area excludes an area between the Colorado River and the Spencer and Hindu Canyons (fig. 1). The Grand Canyon West Development is the only concentration of residents on the western Hualapai Plateau. As of 2010, about 35 full-time residents and an additional 200 seasonal employees were at the development (Hualapai Department of Water Resources, 2010).

Physiography

The Hualapai Plateau ranges in elevation from over 6,000 ft along the Grand Wash Cliffs and Music Mountains to the west, to less than 2,000 ft along the Colorado River and its tributary canyons. The Hualapai Plateau consists of mostly layered sedimentary rocks similar to those found across the Grand Canyon region. The Grand Wash Fault, forming the Grand Wash Cliffs, is the boundary between the Hualapai Plateau and the heavily faulted, folded, and eroded Basin and Range Province to the west (fig. 1). Numerous drainages incise the Hualapai Plateau from southwest to northeast, ending at the Colorado River (fig. 1). The southern boundary of the western Hualapai Plateau is formed by an abrupt change in elevation between the plateau and the Truxton basin (also known as Truxton valley). This abrupt change in elevation is due mainly to the erosion and removal of Paleozoic deposits from the Truxton basin.

Vegetation cover on the western Hualapai Plateau is pinyon-juniper woodland at high elevations. Farther to the southeast along the plateau, vegetation transitions to lower-elevation introduced annual grasslands and native shrublands dominated by sagebrush, saltbush, and Mormon tea. Vegetation in the lower canyon reaches is dominantly desert scrub, such as creosote bush and white bursage (LANDFIRE, 2014).

Climate

The climate of the western Hualapai Plateau ranges from semiarid to arid, which generally correlates to elevation. Average annual temperature, precipitation, and evaporation for the Hualapai Plateau are shown on figure 2 (PRISM Climate Group, 2020). No climate reporting stations are present on the western Hualapai Plateau.

Daily maximum temperatures in higher elevation areas of the western Hualapai Plateau vary from about 45 degrees Fahrenheit (°F) during the winter to about 90 °F during the summer. Daily minimum temperatures vary from about 30 °F during the winter to about 65 °F during the summer. At lower elevations, near the Colorado River, daily maximum temperatures vary from about 60 °F during the winter to about 110 °F during

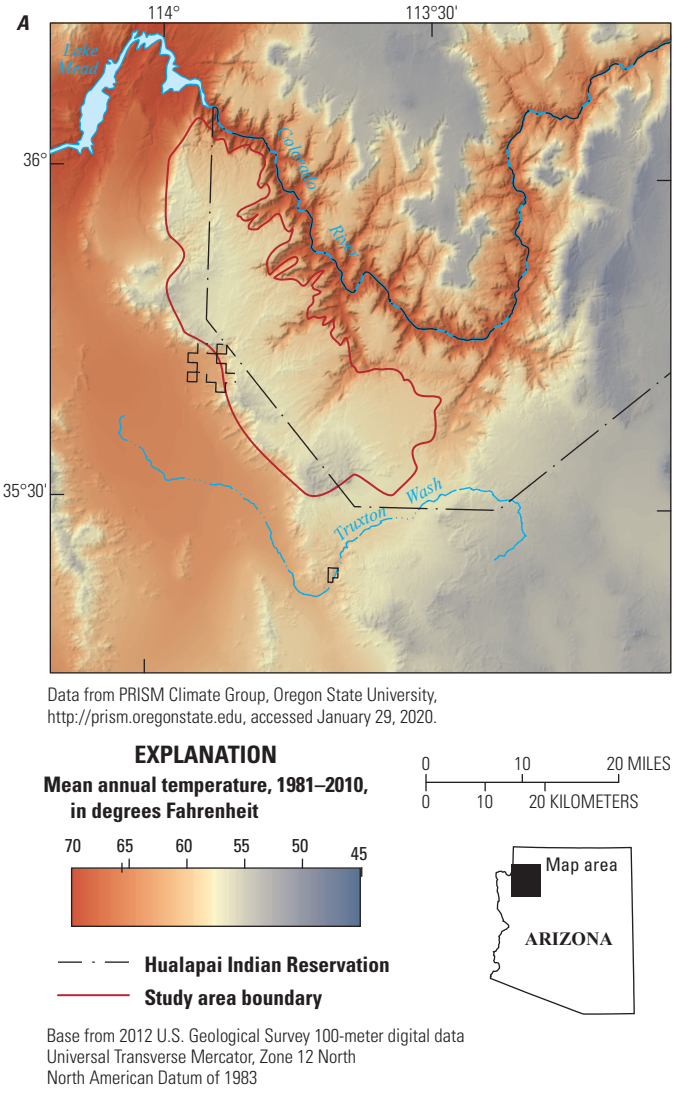

Figure 2 (pages 4–5). Maps of the 30-year mean annual temperature (*A*) and mean annual 30-year precipitation and evaporation of western Grand Canyon (*B*) including the Hualapai Indian Reservation, Arizona.

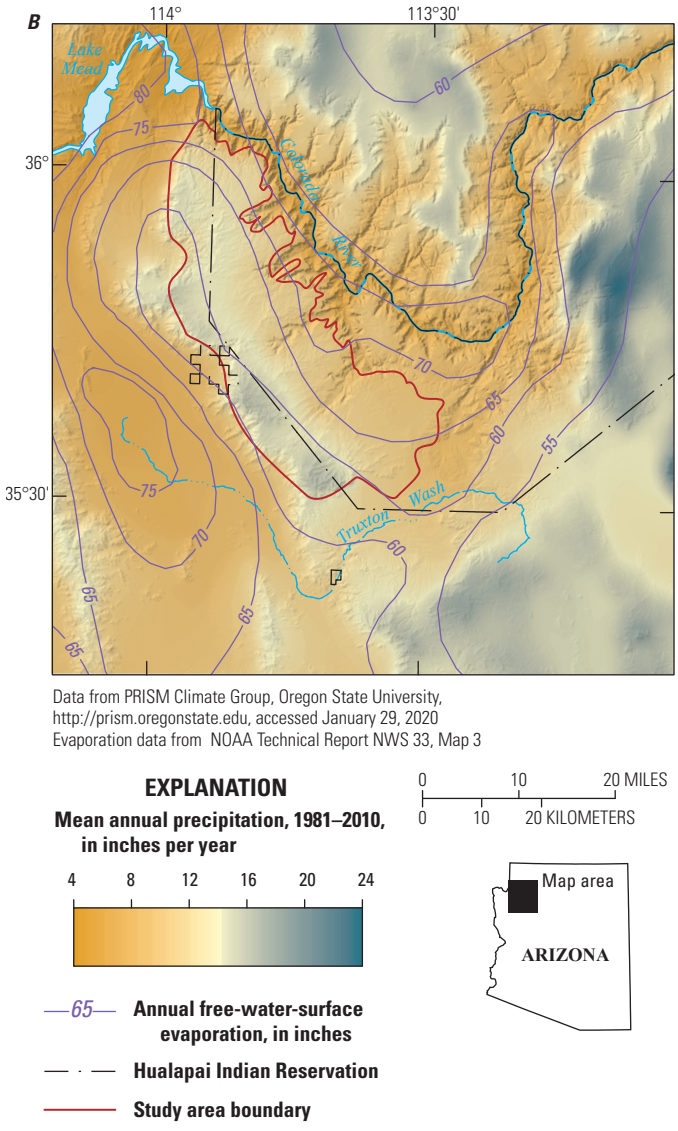

Figure 2 (pages 4–5). —Continued

the summer. Daily minimum temperatures vary from the about 35 °F during the winter to about 75 °F during the summer (PRISM Climate Group, accessed December, 2019, at http://www.prism.oregonstate.edu/). Precipitation comes predominantly from winter storms and summer thunderstorms associated with the North American Monsoon (Adams and Comrie, 1997). Average annual precipitation varies from about 6–8 in/yr along the Colorado River to 10–15 in/yr in higher elevations of the plateau (fig. 2*B*; PRISM Climate Group, 2020). The western Hualapai Plateau, much like the rest of the Southwest, is currently in a long-term drought that began around 2000 (Hereford and others, 2002; Knutson and others, 2007). Evaporation potential for the western Hualapai Plateau has been estimated to be about 60–70 in/yr (Farnsworth and others, 1982), exceeding the average annual precipitation. (fig. 2*B*; Farnsworth and others, 1982).

Geology

The geology of the western Hualapai Plateau consists of Proterozoic crystalline and metamorphic rocks; layered Paleozoic sedimentary rocks; Tertiary to Quaternary (Cenozoic) gravel and fluvial deposits and volcanic rocks; and recent (Holocene) alluvial and travertine deposits. Proterozoic crystalline and metamorphic rocks are primarily exposed at the base of deeply incised canyons and along the Colorado River, its tributaries, and near the base of the Grand Wash Cliffs. Paleozoic sedimentary rocks nonconformably overlie Proterozoic crystalline and metamorphic rocks and consist of steep slope- to cliff-forming layered limestones, shales, siltstones, and sandstones typical of the sequence observed in the western Grand Canyon (figs. 3 and 4). The Tertiary and Quaternary units comprise volcanic rocks as well as gravel and fluvial sediment that form fill deposits in paleochannels that have incised into the Hualapai Plateau. These basin- and paleochannel-fill sediments are semiconsolidated to poorly consolidated, coarse-grained, well-rounded cobbles, gravels, and sands of locally derived sandstones, limestones, and volcanic rocks (Billingsley and others, 1999). Holocene alluvial deposits are found in the stream channels of deeply incised tributaries to the Colorado River. Quaternary travertine occurs at springs with moderate to large flow volumes that discharge from limestone rocks.

Paleozoic strata exposed on the western Hualapai Plateau unconformably overlie Proterozoic crystalline and metamorphic rocks and have a total thickness ranging from 2,930–3,640 feet (ft) (Billingsley and others, 2006). The Cambrian Tapeats Sandstone has a thickness that ranges from about 0 to 200 ft, thinning to the northeast and pinching out a few miles west of the Hurricane Fault. It was deposited unconformably on Proterozoic crystalline and metamorphic rocks. The Cambrian Bright Angel Shale (300 to 350 ft thick) conformably overlies the Tapeats Sandstone and grades upwards into the Cambrian–Devonian Muav Limestone (about 1,200 to 1,400 ft thick). The (unconformably) overlying Temple Butte Formation is 400 to 460 ft thick, where not eroded at land surface. It is uncomfortably overlain by the Mississippian Redwall Limestone that is 630 to about 730 ft thick, where not eroded at land surface. The lower Pennsylvanian Wescogame, Manakacha, and Watahomigi Formations are undivided in this study and are 400 to 500 ft thick, where not eroded at land surface. This undivided unit will be referred to as the lower Supai Group in the rest of the report. The lower Supai Group is found at land surface in the northeastern parts of the western Hualapai Plateau along the western rim of the Grand Canyon and unconformably overlies the Redwall Limestone (figs. 3 and 4) (Billingsley and others, 2006). Paleozoic rocks that underlie the western Hualapai Plateau gently dip to the northeast except where strata are further modified by geologic structure, such as folds, fractures, and faults (fig. 3).

Most of the erosional surfaces of the Hualapai Plateau began forming in response to the regional Laramide uplift of

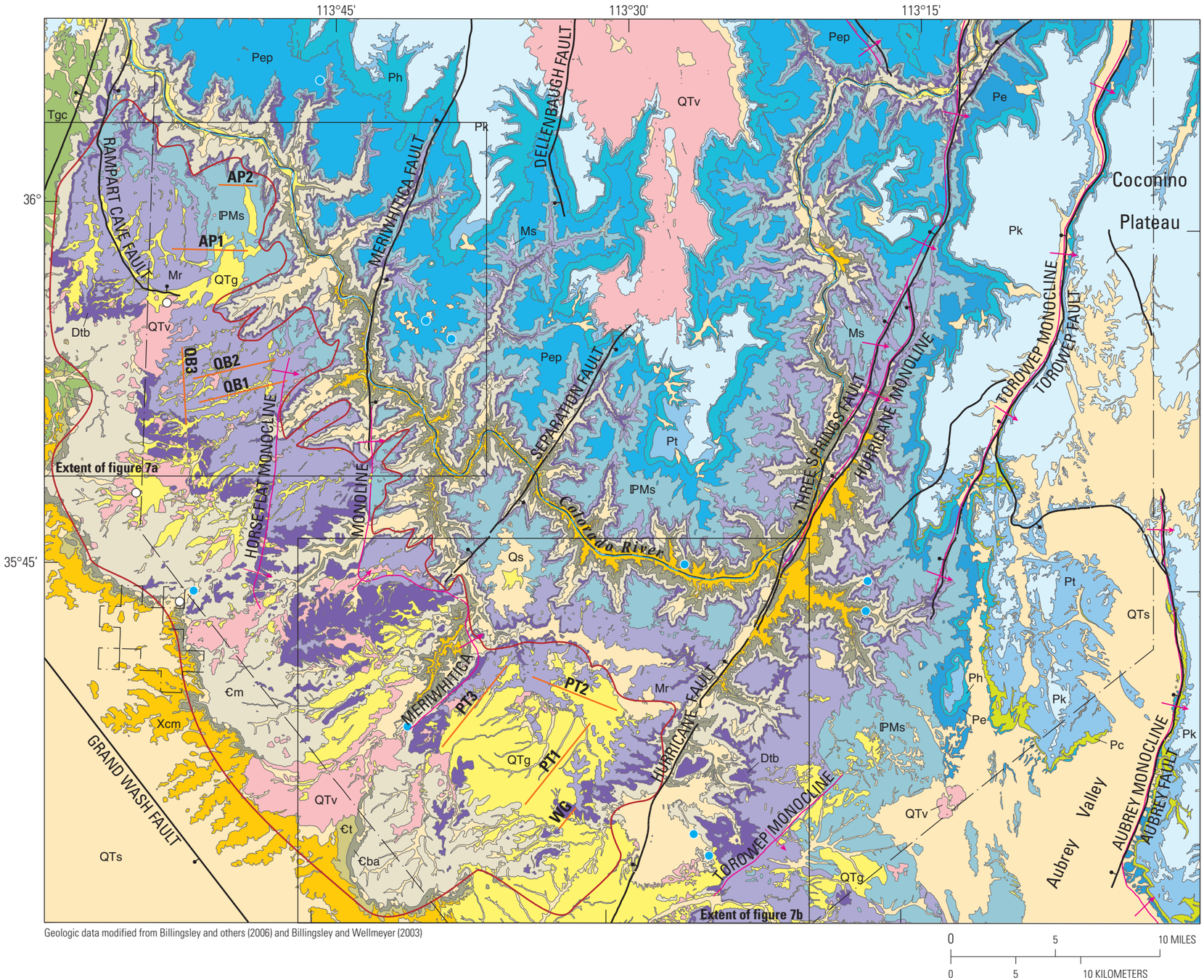

Geologic data modified from Billingsley and others (2006) and Billingsley and Wellmeyer (2003)

EXPLANATION

- QTs — **Surficial deposits, undifferentiated**
- QTg — **Gravel deposits, undifferentiated**
- QTv — **Volcanic rocks, undifferentiated**
- **Cenozoic sedimentary rocks**
- Tgc — Paleozoic-clast conglomerate
- **Paleozoic sedimentary rocks**
- Pk — Kaibab Formation
- Pt — Toroweap Formation
- Pc — Coconino Sandstone, undivided
- Ph — Hermit Formation
- Supai Group
- Pe — Esplanade Sandstone
- Pep — Esplanade Sandstone and Pakoon Limestone
- IPMs — Wescogome, Manakacha, and Watahomigi Formations, undivided
- Ms — Surprise Canyon Formation
- Mr — Redwall Limestone
- Dtb — Temple Butte Formation
- Tonto Group
- Cm — Muav Limestone
- Cba — Bright Angel Shale
- Ct — Tapeats Sandstone
- **Proterozoic rocks**
- Xcm — Crystalline and metamorphic rocks

- **Fault**—Includes approximately located, concealed, or inferred faults. Bar and ball on downthrown block
- **Regional monocline**—Includes approximately located, concealed, or inferred. Showing axial plane and direction of plunge
- **Hualapai Indian Reservation boundary**
- **Study area boundary**
- AP1 — **CSAMT survey line**
- **Well**—Approximately located
- **Spring**—Approximately located

Figure 3. Map of the surface geology and geologic structure of the western Hualapai Plateau in northwestern Arizona (modified from Billingsley and Wellmeyer, 2003; Billingsley and others, 2006). Boxes on the map outline the geographic extent of figures 7*A* and 7*B*.

the southwest Colorado Plateau from the Late Cretaceous to Eocene (Young, 1966, 1987). The uplift resulted in northeast-flowing streams that created deeply incised (1,500 to 2,000 ft deep) paleochannels and paleocanyons, some of which are still visible today. These channels were occasionally dammed with sediments from debris flows and volcanic deposits, allowing the paleochannels to fill with fluvial sediments throughout the late Tertiary until they were again breached. Pulses of erosion have removed much of the fluvial sediment deposited when the canyons were blocked, but some remnants remain today. These remnants consist of poorly sorted, partly consolidated to unconsolidated coarse-grained sandstones and siltstones with gravel, sand, silt, and clay and are 40 to 220 ft thick where exposed (Young, 1999; Billingsley and others, 2006).

Miocene age volcanic rocks on the western Hualapai Plateau often either overlie or intertongue with older Tertiary gravels and sediments. These volcanic rocks are mostly basalts, andesitic basalts, and rhyolite ash flows originating from volcanic necks and dikes along the Grand Wash Cliffs (Young, 1999; Billingsley and others, 2006).

Terrace deposits of sediments and channel alluvium are found in most of the incised drainages on the western Hualapai Plateau. Late Tertiary to early Quaternary sediment deposits and Holocene channel alluvium are a poorly sorted and unconsolidated to partly consolidated mix of clay, silt, sand, pebbles, cobbles, and small boulders. These units range from about 10 to 260 ft thick in the bottom of most drainages. These deposits are typically reworked older and younger coarse sediment units and locally sourced volcanic rocks that are subject to sporadic deposition and erosion from flashflood and debris-flow events (Billingsley and others, 2006). For simplicity, Quaternary and Tertiary deposits other than gravel have been combined into a single geologic unit called surficial deposits, undifferentiated (QTs), and Quaternary and Tertiary gravel units have been combined into a geologic unit called gravel deposits (QTg).

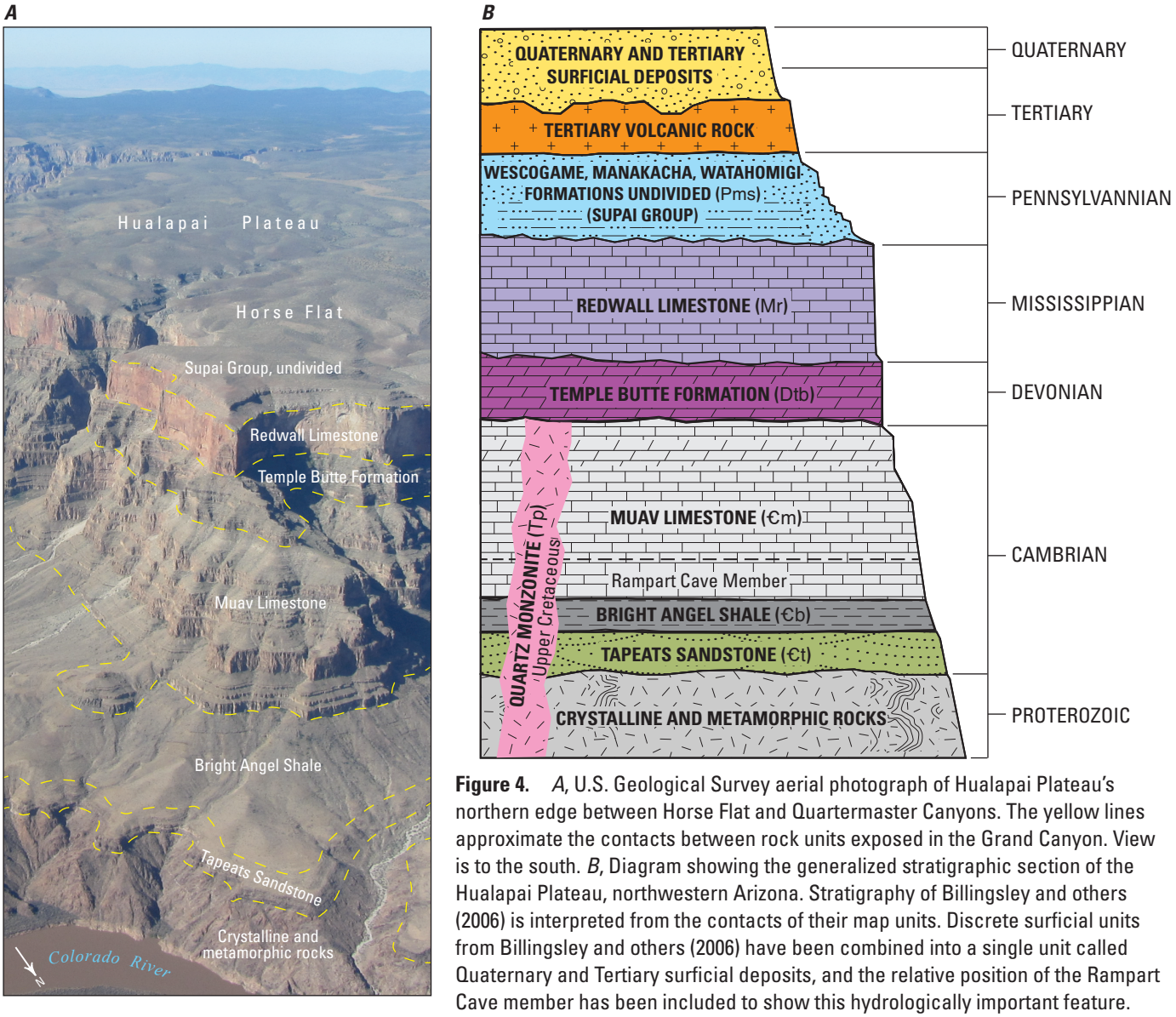

Figure 4. *A*, U.S. Geological Survey aerial photograph of Hualapai Plateau's northern edge between Horse Flat and Quartermaster Canyons. The yellow lines approximate the contacts between rock units exposed in the Grand Canyon. View is to the south. *B*, Diagram showing the generalized stratigraphic section of the Hualapai Plateau, northwestern Arizona. Stratigraphy of Billingsley and others (2006) is interpreted from the contacts of their map units. Discrete surficial units from Billingsley and others (2006) have been combined into a single unit called Quaternary and Tertiary surficial deposits, and the relative position of the Rampart Cave member has been included to show this hydrologically important feature.

Pleistocene and Holocene age travertine deposits crop out in incised canyons of the western Hualapai Plateau where springs discharge from the Rampart Cave Member of the Muav Limestone, located at the bottom of the Muav Limestone (Billingsley and others, 2006). The thickest deposits occur in Meriwhitica, Spencer, Travertine, and Quartermaster Canyons, where travertine is still actively being deposited and travertine dams have developed. The thickness of the travertine deposits ranges from about 6 to over 200 ft.

Geologic structures are significant to the groundwater resources of the western Hualapai Plateau, because they affect the occurrence and movement of groundwater and groundwater-storage potential (Young, 1978). Some geologic structures offset the elevation of impermeable Proterozoic crystalline and metamorphic bedrock, which alters potential storage space and can impede groundwater flow. Faulted and folded structures can be either conduits or barriers to groundwater flow depending on the type and activity of the structures and the lithology of surrounding rock units. Geologic features can affect the local water quality by creating pathways for surface contaminants to enter the aquifer. Groundwater yield may also be affected by geologic features that create or impede flow paths.

Complex geologic structures occur in and adjacent to the western Hualapai Plateau. In general, most faults are high angle to nearly vertical and have a normal component of displacement. Regional contraction and uplift of the Colorado Plateau began in the Late Cretaceous and resulted in several monoclinal, generally east dipping folds (Billingsley and others, 2006). Ongoing uplift through the early Tertiary at the western margin of the Colorado Plateau resulted in reverse fault motion on basement faults. This motion has propagated upward varying distances into the Paleozoic rocks and has further stimulated folds, although these features have not always been expressed at the surface. The principal geologic structures on the western Hualapai Plateau are the Hurricane Fault, the Meriwhitica Monocline and Fault, the Separation Fault, the Horse Flat Monocline and Fault, the Rampart Cave Fault, and the Grand Wash Fault (Wenrich and others, 1996; Billingsley and others, 2006). Numerous smaller, unnamed faults, anticlinal and synclinal structures, and collapse features are scattered across the western Hualapai Plateau (fig. 3).

The Grand Wash and Hurricane Faults are the largest structural features associated with the western Hualapai Plateau. The Grand Wash Fault is a northwest-southeast striking, high-angle, normal fault that extends from southwestern Utah to northwestern Arizona. It forms the western and southwestern boundary of the Hualapai Plateau and, in this region, separates the Basin and Range physiographic province from the Colorado Plateau Province. Lucchitta (1967) reported the displacement of the fault near the Colorado River could be as much as 16,000 feet.

The Hurricane Fault is a 150-mile-long, north-south striking, high-angle normal fault that extends across southwestern Utah and northwestern Arizona about 20 to 40 miles east of the Grand Wash Fault (Stewart and others, 1997). The fault trends northeast to southwest along Peach Springs Canyon at the southeast edge of the western Hualapai Plateau (figs. 1 and 3). The eastern side of the fault has a component of upward displacement that ranges from about 1,600 ft near the Colorado River to about 210 ft at the upper end of Peach Springs Canyon (Billingsley and others, 2006). For much of the length of the fault in Peach Springs Canyon, this displacement places Proterozoic crystalline and metamorphic basement rock to the east of the fault opposite Paleozoic and younger rocks on the west side of the fault. How this fault affects groundwater flow is unknown, but faults are often barriers or conduits of flow.

Hydrology and Hydrogeology

The hydrology and hydrogeology of the western Hualapai Plateau are poorly understood in spite of studies conducted since the 1960s. In particular, data are limited on water use, wells, and flow for both surface-water and groundwater resources in the area. Most surface-water drainages on the western Hualapai Plateau are ephemeral or intermittent. Perennial reaches are typically supported by groundwater discharge from springs, which are the most significant source of surface water on Hualapai Plateau lands outside of the Colorado River. However, many of the springs are in remote, deeply incised canyons that limit their access and make it difficult to determine origin of flow, flow variability, and water quality. Most of the groundwater wells on the western Hualapai Plateau are screened-in, shallow perched water-bearing material associated with basin-fill sediments or volcanic rocks. Prior to this study, only the deep well near Grand Canyon West (GCW-1) was drilled into bedrock on the western Hualapai Plateau (Watt, Bureau of Reclamation, written commun., 2000).

The principal drainages of the western Hualapai Plateau from southeast to northwest are Peach Springs Canyon, Spencer creek (including Milkweed, Meriwhitica, and Hindu Canyons), Lost Creek (Clay Tank Canyon), Reference Point Creek (Horse Flat Canyon), and Quartermaster Canyon (fig. 1). Discharge and water-quality information from springs located in these five drainages, as well as in other areas on and adjacent to the western Hualapai Plateau, can be found in table 2.1 of appendix 2.

The occurrence and movement of groundwater in the western Hualapai Plateau are strongly influenced by the porosity, permeability, lithology, and geologic structure of the surrounding rock. The lithology of geologic units changes both laterally and vertically across the western Hualapai Plateau, affecting the porosity and permeability across and within geologic units. Geologic structures on the western Hualapai Plateau include fractures, faults, and folds that alter the position of geologic units and create secondary permeability that can considerably increase groundwater flow.

Usable groundwater on the western Hualapai Plateau is in either perched water-bearing zones close to land surface (paleochannel-fill sediments, volcanic rocks, and (or) recent

channel alluvium) or in the Muav Limestone at depths greater than 2,000 ft below land surface (Twenter, 1962). A series of discontinuous paleochannel-fill sediments and volcanic rocks cross the western Hualapai Plateau from southwest to northeast. Miocene basalt flows are found at land surface and in paleochannels where they are interbedded between the older and younger sediments that continued to fill these channels through the Pliocene (Billingsley and others, 2006). The most productive of these perched water-bearing zones are in the Milkweed Canyon and West Water Canyon drainages where several springs discharge tens to over 100 gal/min. The remaining perched paleochannel water-bearing zones in the upper ends of various canyons in the area do not have sufficient storage to support springs. However, the Hualapai Tribe has developed a few shallow windmill wells in these areas to provide water for livestock and wildlife.

Groundwater in the Muav Limestone is found near the bottom of the geologic unit in the Rampart Cave Member. In some parts of northern Arizona, the Muav Limestone is considered part of the Redwall-Muav multiple aquifer system (Cooley, 1976). The Redwall-Muav aquifer is a large regional groundwater-flow system that underlies most of northern Arizona from the Mogollon Rim to the Utah border and consists of the Redwall Limestone, Muav Limestone, and the Temple Butte Formation (Cooley, 1976; Bills and others, 2007). The term Muav aquifer, instead of Redwall-Muav aquifer, is used in this report because water is more commonly found in the Muav Limestone than the Redwall Limestone or Temple Butte Formation. The Colorado River has cut this regional aquifer roughly in half (by the Grand Canyon), and most of the major springs on the northern edge of the Hualapai Plateau discharge from the Muav aquifer. Karst features in limestones are common within the western Hualapai Plateau and include collapse structures, sinkholes, and breccia pipes (Billingsley and others, 1999). The depth to groundwater in the Muav aquifer of the western Hualapai Plateau is greater than 2,000 ft below land surface, which is assumed on the basis of most Muav aquifer springs' elevation along the Colorado River.

The highest elevation area on the western Hualapai Plateau is the Music Mountains, which is the uplifted block of the Grand Wash Fault located and buried to the west in Hualapai Valley. The maximum topographic relief in this area of the Grand Wash Fault is about 4,000 ft and the uplifted portion has a shallow regional east to northeast dip (Billingsley and others, 2006). This regional dip along with east-west facies and thickness changes of Paleozoic rocks on the western Hualapai Plateau are important components of recharge, storage capability, and the occurrence and movement of groundwater. Because the structural dip is greater than the topographic slope, the Muav Limestone is exposed at higher elevations in the Grand Wash Cliffs and is therefore likely to recharge in that area. Regional groundwater flow is assumed to be from the southwest to northeast, on the basis of the regional dip and the abundance of springs in the Grand Canyon and lack of them in the Grand Wash Cliffs. Because the Hualapai Plateau is surrounded by cliffs on the north, west, and south sides, and the Hurricane Fault on the east side, it is likely hydrologically isolated from the rest of the Colorado Plateau.

Spencer and Meriwhitica drainages are known to have perched water-bearing zones in paleochannels that occur at higher elevations. In West Water and Upper Milkweed Canyons (fig. 1), several springs occur where erosion and downcutting have exposed the lower contact of the paleochannels with underlying volcanic rocks or the Muav Limestone. Eagle spring (an informally named spring southeast of Milkweed Canyon), Spencer Springs, and Meriwhitica Springs discharge from the Muav Limestone in the Spencer creek drainage. Three discharge measurements made at Eagle spring in the 1990s ranged from dry to 1,023 gal/min, and two discharge measurements from Meriwhitica Springs were 1,230 and 7,315 gal/min in the 1990s. No measurements are available from Spencer Springs.

The USGS has operated a streamflow-gaging station (09404222) on Spencer creek near Peach Springs, Ariz., since 1998 (fig. 1). A winter-baseflow evaluation from the 20 years of record available from the gage was attempted. However, because of occasional winter precipitation runoff events, using winter flow as a surrogate measurement for baseflow was not possible. Figure 5 shows the median winter flow (November through February) at the gage for water years 1999–2018. The median was used since it was less affected by occasional winter runoff. The average of these annual median flows is 3.3 cubic feet per second (ft^3/s; fig. 5). This is not an actual measurement of baseflow, but it serves as a reference for the approximate magnitude of what baseflow is likely to be.

Natural Resources Consulting Engineers (2011) used the Maxey-Eakin (1949) method to determine an annual groundwater recharge of about 3 percent of the average annual precipitation for the reservation, with the greatest groundwater recharge occurring in mountain-front areas like the Music Mountains at the north end of the Truxton basin. Earlier estimates of recharge were lower (Devlin, 1976; Huntoon, 1977), likely because they assumed all recharge discharges at springs and because they disregarded evapotranspiration (ET) derived from near-surface groundwater adjacent to the spring (Natural Resources Consulting Engineers, 2011).

More recently, annual runoff estimates were developed for the Peach Springs Basin by Tillman and others (2011) using Parameter-Elevation Relationships on Independent Slopes Model (PRISM) data as the basis for precipitation, a Basin Characterization Model (BCM; Flint and Flint, 2007a, b), and a multiple-regression equation to estimate runoff and recharge. The western Hualapai Plateau is part of the Peach Springs Basin and makes up about two thirds of the basin area. The average annual groundwater recharge estimate for the Peach Springs Basin, determined by the BCM was about 0.32 inches (in.) or about 3 percent of the annual average precipitation of 11.9 in/yr.

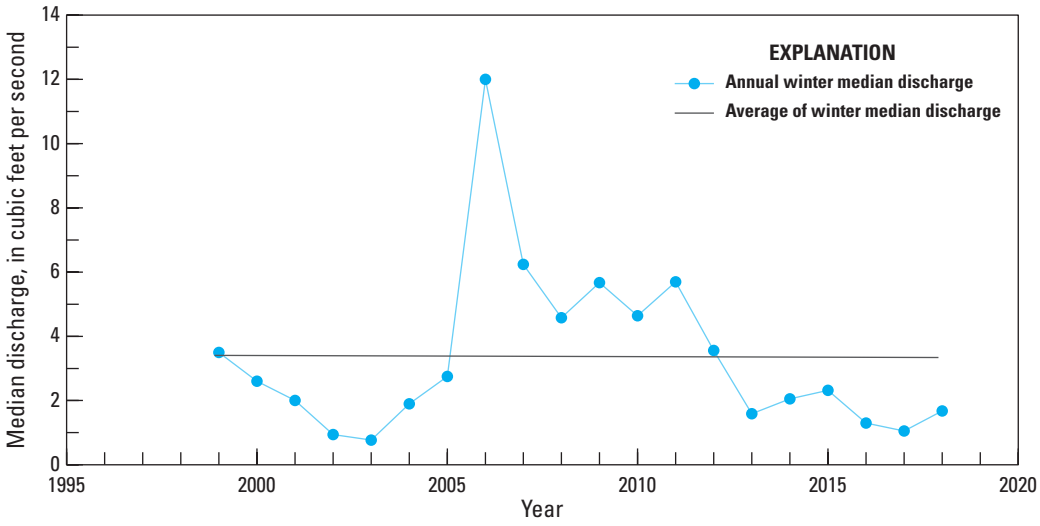

Figure 5. Graph showing the winter median discharge (November to February) from 1999–2018 for the U.S. Geological Survey streamflow-gaging station Spencer creek near Peach Springs, Ariz. (09404222).

Methods

This study used ground-based geophysical surveys combined with existing well, spring, and other hydrogeologic information available from previous studies and new well and spring data collected for this study, to develop a better understanding of the hydrogeology of the western Hualapai Plateau. Controlled source audio-frequency magnetotellurics (CSAMT) was chosen as the best-suited geophysical method for this study. Existing well, water-level, spring, and new hydrogeologic information from well and spring inventories of the western Hualapai Plateau were used to update the conceptual understanding of both bedrock and perched aquifers.

Controlled Source Audio-Frequency Magnetotelluric Surveys

CSAMT is an electromagnetic sounding technique that has proven useful for hydrogeological and groundwater studies (Zonge, 1992). CSAMT measures electrical resistivity in the subsurface to depths of about 3,000 meters (m) (9,800 ft) below land surface. Because the electrical resistivity varies with rock types and water content, this method may provide an indication of subsurface structure (strata, faults, and fractures) and the presence of groundwater (Simpson and Bahr, 2005). This low-impact, nonintrusive technique has been used extensively by the mineral, geothermal, hydrocarbon, and groundwater exploration industries since 1978 when CSAMT equipment systems first became commercially available (Zonge, 1992).

The CSAMT method provides the electrical resistivity of the subsurface along a receiver profile. This is accomplished by measuring electric and magnetic fields introduced into the Earth by a controlled current transmitted at several frequencies a specified distance away (fig. 6). Grounded dipoles at the receiver site detect the electric field parallel to the transmitter, and a magnetic-coil antenna senses the magnetic field perpendicular to the transmitter (fig. 6). The ratio of the orthogonal and horizontal electric-field magnitudes to magnetic-field magnitudes yields the apparent resistivity. CSAMT uses a remote, grounded, electric-dipole transmitter as an artificial signal source. The transmitter source provides a stable signal, resulting in higher precision and faster measurements than can be obtained from natural source audio-frequency magnetotellurics (Zonge, 1992). Typically, the source for a CSAMT survey is separated from the survey line by about five times the depth of investigation because a plane wave is advantageous (fig. 6).

CSAMT measurements typically are made at frequencies ranging from 1 to 8,000 hertz in binary incremental steps. The frequencies used for the surveys in this report were 2, 4, 8, 16, 32, 64, 128, 256, 512, 1,024, 2,048, 4,096, and 8,192 hertz. CSAMT measurements consist of orthogonal and parallel components of the electric (E) and magnetic (H) fields at a separation of 5 to 15 kilometers (km, 3.1 to 9.3 mi) from the source (Sharma, 1997). CSAMT measurements can be taken in several different arrays depending on the type of information desired. This study used what is termed a “reconnaissance” type of CSAMT array, which consists of one electric (E_x) and one magnetic (H_y) component for each measurement (Zonge, 1992), as opposed to a more involved survey, which collects vector and tensor measurements by measuring two electric-field components (E_x and E_y) and three magnetic-field components (H_x, H_y, and H_z). Multiple electric fields are measured concurrently during reconnaissance CSAMT surveys.

This study used a six-channel receiver, with the capability of simultaneously measuring five electric fields for every one magnetic field. Fewer magnetic-field measurements are required than electric-field measurements because the magnetic field does not change much over the same distance that substantial electric-field changes occur. The magnetic-field measurement is used to normalize the electric-field measurements and calculate the apparent resistivity and phase difference (Zonge, 1992). Grounded dipoles at the receiver site measure the electric field parallel to the transmitter (E_x), and a magnetic coil antenna

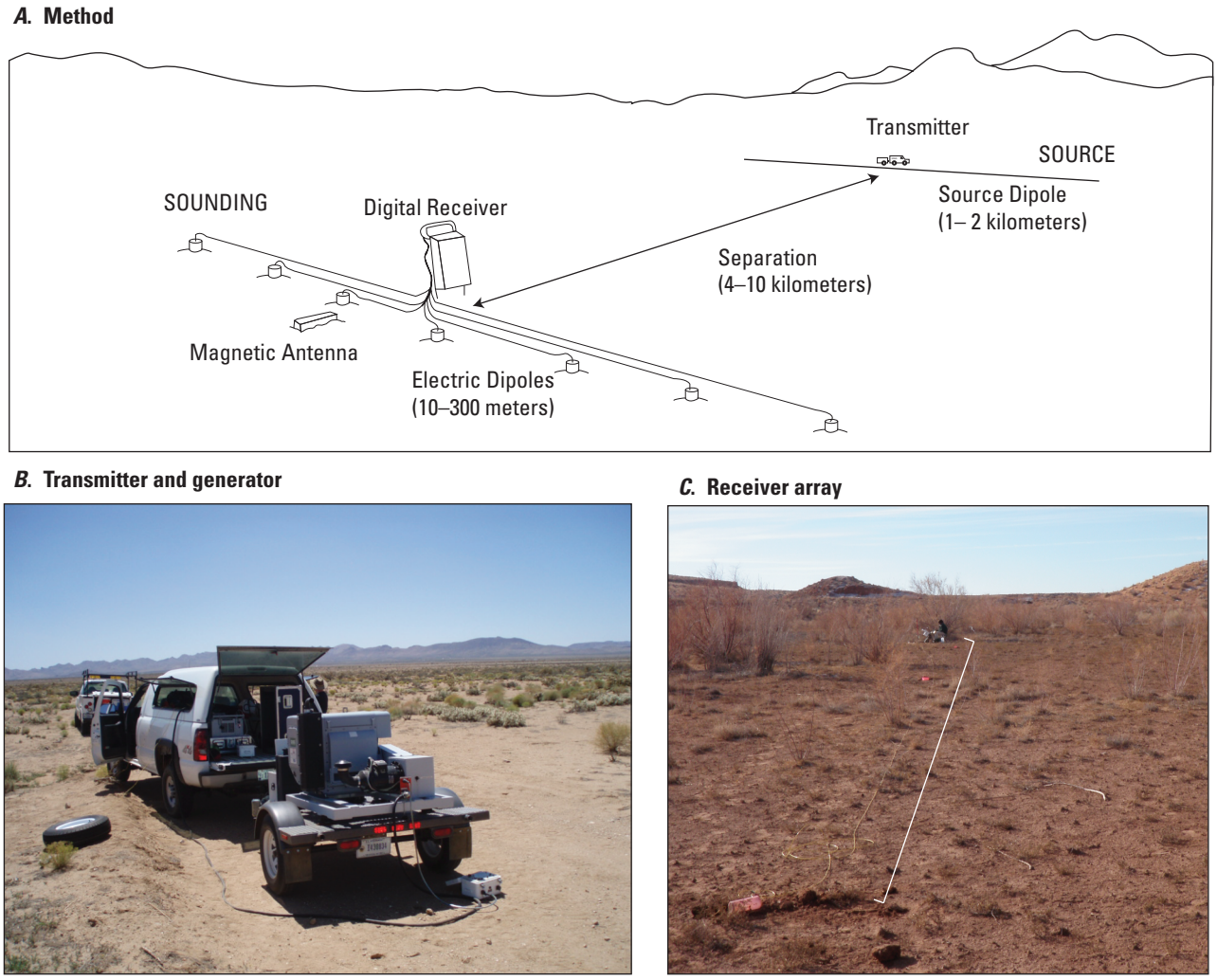

Figure 6. Diagram (*A*) and photographs (*B, C*) showing controlled source audio-frequency magnetotelluric setup used to study the western Hualapai Plateau, northwestern Arizona. Diagram modified from Zonge (1992); photographs by D.J. Bills and Jon Mason of the U.S. Geological Survey.

measures the perpendicular magnetic field (H_y). The ratio of the E_x and H_y magnitudes yields the apparent resistivity (equation 1; Zonge, 1992; Simpson and Bahr, 2005):

$$\rho_a = \frac{1}{5} f \left[\frac{E_x}{H_y} \right]^2 \quad (1)$$

where

ρ_a is the apparent resistivity,
f is the frequency,
E_x is the parallel electrical-field strength, and
H_y is the perpendicular magnetic-field strength.

The skin depth is the depth at which the amplitude of a plane wave signal has dropped to 37 percent of its value at the surface (Zonge, 1992). The skin depth is pertinent because CSAMT data are most commonly interpreted using simplified magnetotelluric (MT) equations based on the assumption that the electric and magnetic fields behave as plane waves.

Unlike MT soundings, where the source of telluric current (distant lightning strikes or atmospheric interaction with solar winds) is considered infinitely distant and nonpolarized, the CSAMT source is finite in distance and distinctly polarized (Sharma, 1997). The separation, *r*, between the transmitter and receiver for CSAMT surveys must be greater than three skin depths (in the "far field") for the current driven into the ground to behave like plane waves. When *r* is less than three skin depths at the frequency being measured (in the "near field"), the electric and magnetic fields no longer behave as plane waves and become curved such that the equation for apparent resistivity (equation 1) no longer applies. CSAMT measurements from this study were examined for near- and far-field effects before modeling by plotting the apparent resistivity versus the frequency for a given set of soundings. All data from this study used for modeling are measured in the far field. The minimum distance between the source and receiver was 5 km (3.1 mi), yielding an *r* of greater than three skin depths (Zonge, 1992).

When the *r* between the receiver and transmitter is greater than three skin depths, the equation for depth of investigation is the following (Zonge, 1992):

$$D = 356\sqrt{\rho_a \div f} \quad (2)$$

The depth of investigation (D) of a CSAMT survey can range from 20 to 3,000 m (66 to 9,800 ft), depending on the resistivity of the ground and the frequency of the signal. Lower frequency signals have a greater depth of investigation than higher frequency signals.

Collection of Controlled Source Audio-Frequency Magnetotelluric Data

CSAMT data were collected in the Grand Canyon West and Plain Tank Flat areas on the western Hualapai Plateau from August 2017 to November 2017. A Zonge GGT-30 geophysical transmitter and a Zonge XMT-32 transmitter controller were used to transmit the electrical source through a 1-kilometer-long (0.62-mi) dipole. A Zonge GDP-32II multichannel geophysical receiver was connected to six porous pot electrodes arranged in 100-m (328-ft) dipoles and a Zonge ANT6 high-gain mu-metal core magnetic antenna to measure the Earth's response to the transmitted signal. Each CSAMT field measurement consisted of one magnetic-field measurement (H_y) with five accompanying electric-field measurements (E_x).

Nine CSAMT lines, 52.5 km in total length, were surveyed in the Grand Canyon West area and Plain Tank Flat—AP1, AP2, QB1, QB2, QB3, PT1, PT2, PT3, and WG (fig. 7). The separation between transmitter and receiver locations ranged from about 5 to 15 km. Data were processed and analyzed using the DATPRO software suite (CSAVG version 1.10E; SCSD version 3.20R). Raw CSAMT data were first averaged using the program CSAVG. Averaged data were reviewed for near-field and far-field effects by plotting the apparent resistivity versus the frequency (equation 2)

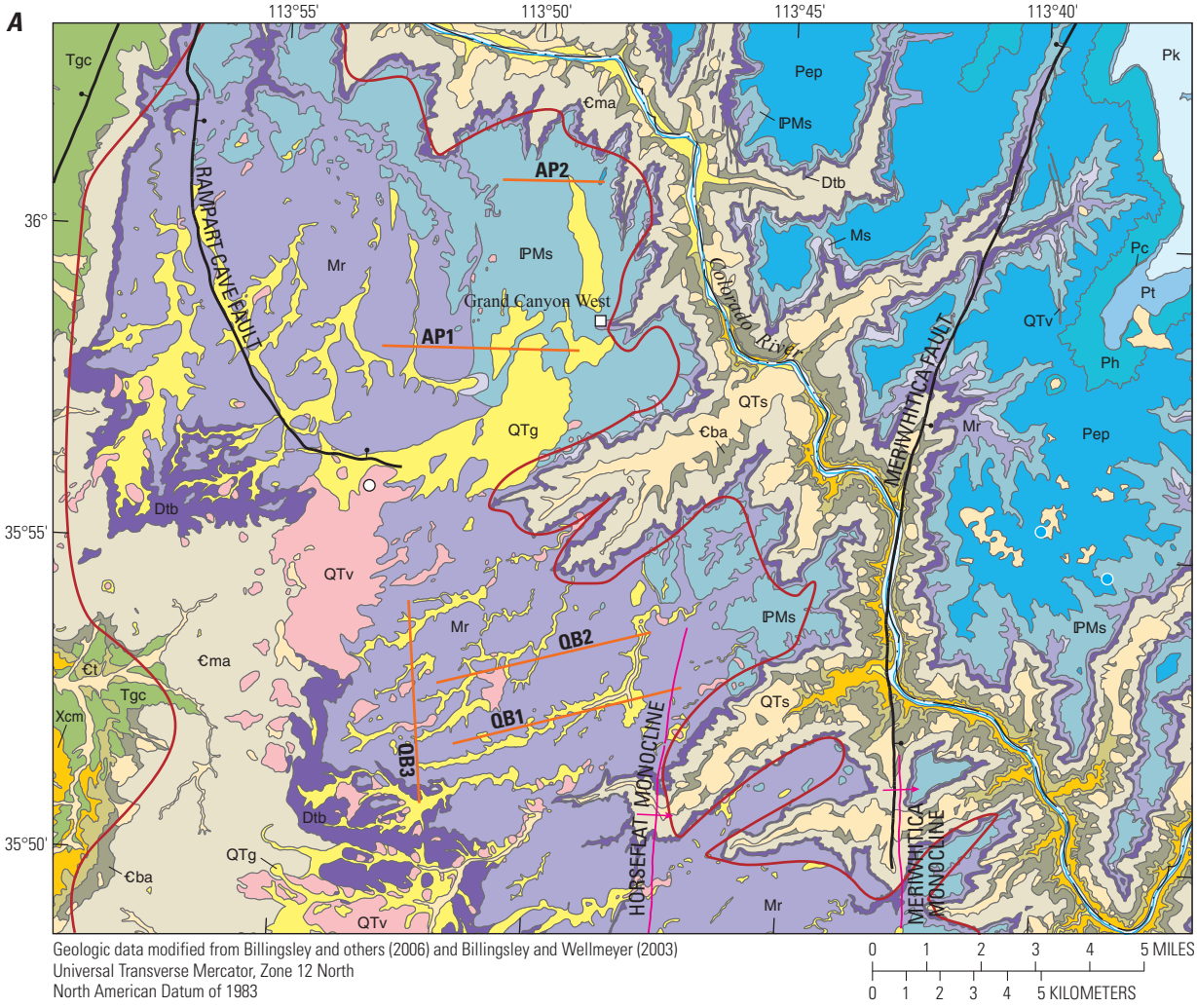

Figure 7 (page 13–14). Surface geology map showing location of controlled source audio-frequency magnetotelluric (CSAMT) soundings on the western Hualapai Plateau, northwestern Arizona. *A*, Location of CSAMT lines in the Grand Canyon West (AP) and Quartermaster to Horse Flat Canyons (QB) area. *B*, Location of CSAMT survey lines in the Plain Tank Flat (PT) and Truxton aquifer (WG) areas.

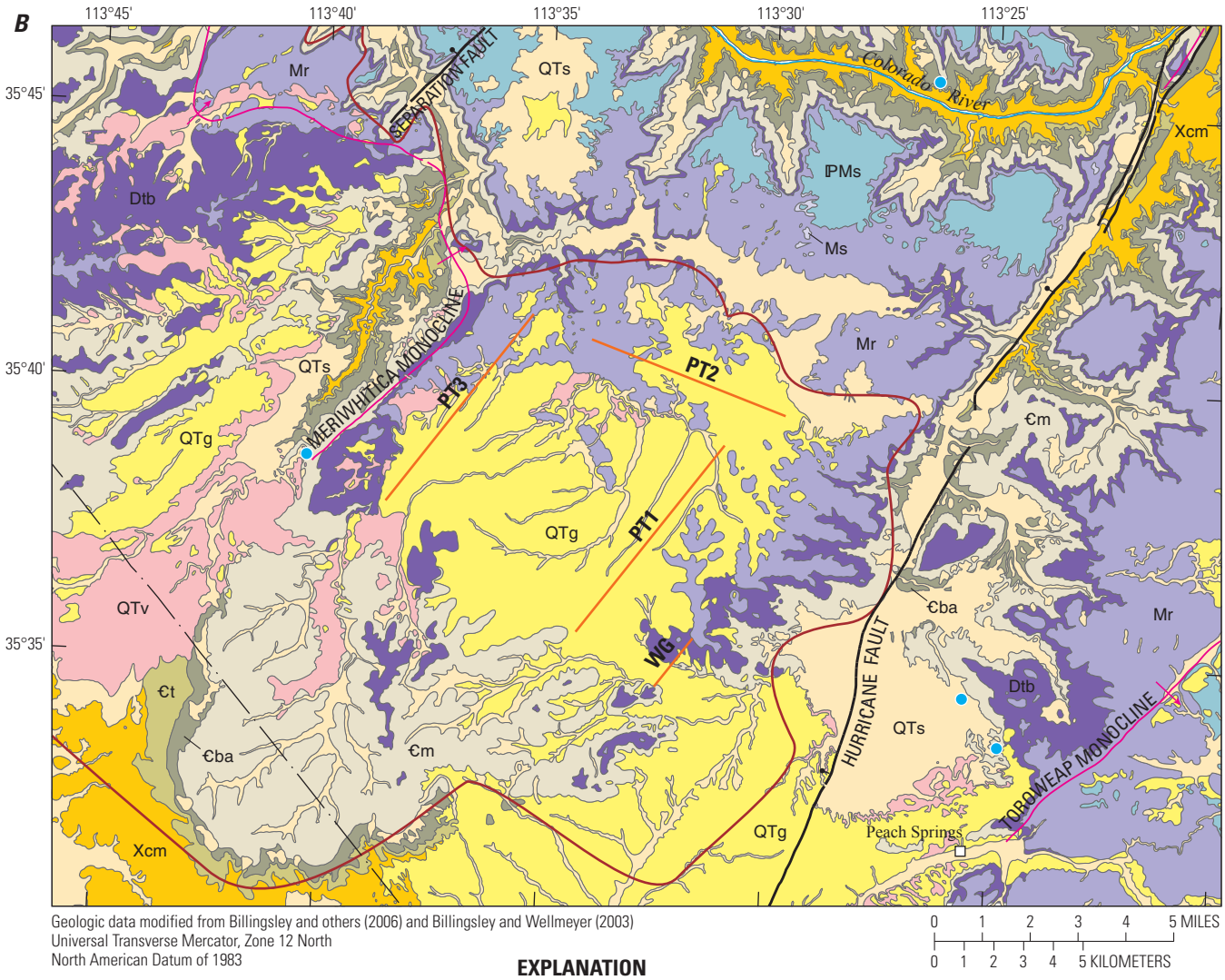

Geologic data modified from Billingsley and others (2006) and Billingsley and Wellmeyer (2003)
Universal Transverse Mercator, Zone 12 North
North American Datum of 1983

0 1 2 3 4 5 MILES
0 1 2 3 4 5 KILOMETERS

EXPLANATION

- QTs — **Surficial deposits, undifferentiated**
- QTg — **Gravel deposits, undifferentiated**
- QTv — **Volcanic rocks, undifferentiated**

Cenozoic sedimentary rocks

- Tgc — Paleozoic-clast conglomerate

Paleozoic sedimentary rocks

- Pk — Kaibab Formation
- Pt — Toroweap Formation
- Pc — Coconino Sandstone, undivided
- Ph — Hermit Formation
- Supai Group
  - Pep — Esplanade Sandstone and Pakoon Limestone
  - IPMs — Wescogome, Manakacha, and Watahomigi Formations, undivided
- Ms — Surprise Canyon Formation
- Mr — Redwall Limestone
- Dtb — Temple Butte Formation
- Tonto Group
  - €m — Muav Limestone
  - €ba — Bright Angel Shale
  - €t — Tapeats Sandstone

Proterozoic rocks

- Xcm — Crystalline and metamorphic rocks

- **Fault**—Includes approximately located, concealed, or inferred faults. Bar and ball on downthrown block
- **Regional monocline**—Includes approximately located, concealed, or inferred. Showing axial plane and direction of plunge
- **Hualapai Indian Reservation boundary**
- **Study area boundary**
- AP1 — **CSAMT survey line**
- **Well**—Approximately located
- **Spring**—Approximately located

Figure 7 (page 13–14). —Continued

for a given set of soundings. The lowest far-field frequency that satisfied the plane wave approximation was determined, and data below that frequency were not used in the analysis. Typically for the surveys in the Grand Canyon West and Plain Tank areas, data from 32 to 8,192 hertz were useful. Data were inverted using the program SCS2D to provide a two-dimensional resistivity profile for each survey line. The profiles were then examined for errors and adjusted as appropriate. Topography was added to each inverted profile after inversion, and additional adjustments were made to the inversion models in areas where the subsurface geology was known from lithologic logs for wells. Final inversion models presented in the "Results" section of this report represent the best fit to subsurface resistivity. All CSAMT supporting the interpretations in this report are publicly available (Macy, 2019).

Collection of Test Well Data

The Hualapai Test Well, hereafter referred to as the test well, was drilled by the USGS on the western Hualapai Plateau with support from the Hualapai Tribe (fig. 1). The test well was drilled and developed to collect information about the subsurface geology and resistivity of geologic units that could be used to compare and verify results of ground-based geophysical data, as well as to evaluate the presence and availability of usable groundwater from bedrock aquifers on the western Hualapai Plateau. The location of the test well—about 4 km northwest of upper Horse Flat Canyon—was selected using geologic maps, spring data in both Horse Flat and Quartermaster Canyons, and ground-based geophysical data collected for this study.

Borehole drilling began on August 9, 2018, and was completed on October 12, 2018. The air hammer method was used with water and foam as the drilling fluid. A 12.0-inch diameter surface casing was set in an 18.0-inch diameter borehole to a depth of 30 ft, and the surface casing was set in concrete and sealed at the surface (fig. 8). The borehole was drilled to a depth of 2,000 ft with a 12-inch diameter air hammer. Geophysical logs consisting of caliper, gamma, and deviation were collected for this portion of the borehole, then a 6-inch solid casing was set in the borehole from land surface to 2,000 ft and cemented and grout sealed in place. The borehole was continued to a total depth of 2,468 ft with a 6-inch diameter air hammer bottoming in about 8 ft of Proterozoic granite (fig. 8). USGS hydrologists collected borehole cuttings at 20-ft intervals from the land surface to 2,468 ft depth (5,123 and 2,655 ft above sea level, respectively). After well construction, a suite of geophysical logs was collected in the open portion from 2,000 to 2,468 ft including caliper, natural gamma, deviation, temperature, specific conductance, spontaneous potential, and short and long resistivity. The geophysical logs (fig. 8) and a detailed lithologic log for the borehole are in table 1.1 of appendix 1 and is publicly available via the USGS GeoLog Locator (https://webapps.usgs.gov/GeoLogLocator/#!/).

A 48-hour, constant-rate pumping and recovery test was conducted between October 20, 2018, and October 24, 2018. Prepumping depth to water below land surface in the well was 1,468 ft. Drawdown and recovery data were collected using a vented pressure transducer attached to the column pipe and set to collect data every 10 seconds for the duration of the test. Temperature of the test well was recorded with a transducer in the well and with a calibrated temperature probe at the well head.

The drawdown and recovery data were used to estimate the transmissivity, hydraulic conductivity, and storativity of the aquifer in the region surrounding the test well. These aquifer properties were estimated using the Papadopulos and Cooper solution for nonleaky confined aquifers (Papadopulos and Cooper, 1967). The pumping and recovery water-level data were processed using AQTESOLV (Duffield, 2007).

The transducer measuring drawdown and recovery was set at about 1,685 ft below land surface, about 130 ft above the pump intake. Check measurements of the recorded water-level data were not made owing to the lack of space in the casing for an electric well probe. Data for recovery were recorded until the water level reached 97 percent of the predrawdown level. No wells were nearby to use as observation wells. Well discharge was measured volumetrically about every hour with a calibrated 5-gallon bucket at the end of a flexible 2-inch water line running from the pump to an earthen stock tank located about 300 ft to the north of the well. The pumping rate was about 6.1 gal/min for the first 96 minutes of the test and about 4.4 gal/min for the remainder of the test. The average pumping rate for the test was about 4.5 gal/min and the total drawdown was 205 ft.

Water-quality field parameters (water temperature, specific conductance, pH, and dissolved oxygen) were collected during the pumping test at 5- to 10-minute intervals (table 1.2 of appendix 1). Near the end of the pumping test, a water-quality sample was collected at the well head for analysis of major ions, trace elements, and stable and environmental isotopes (table 1.3 of appendix 1). Approximately 11,000 gallons of water were pumped from the well prior to the start of sample collection. The water-quality sample was collected using methods described in the USGS National Field Manual for the Collection of Water-Quality Data (U.S. Geological Survey, variously dated).

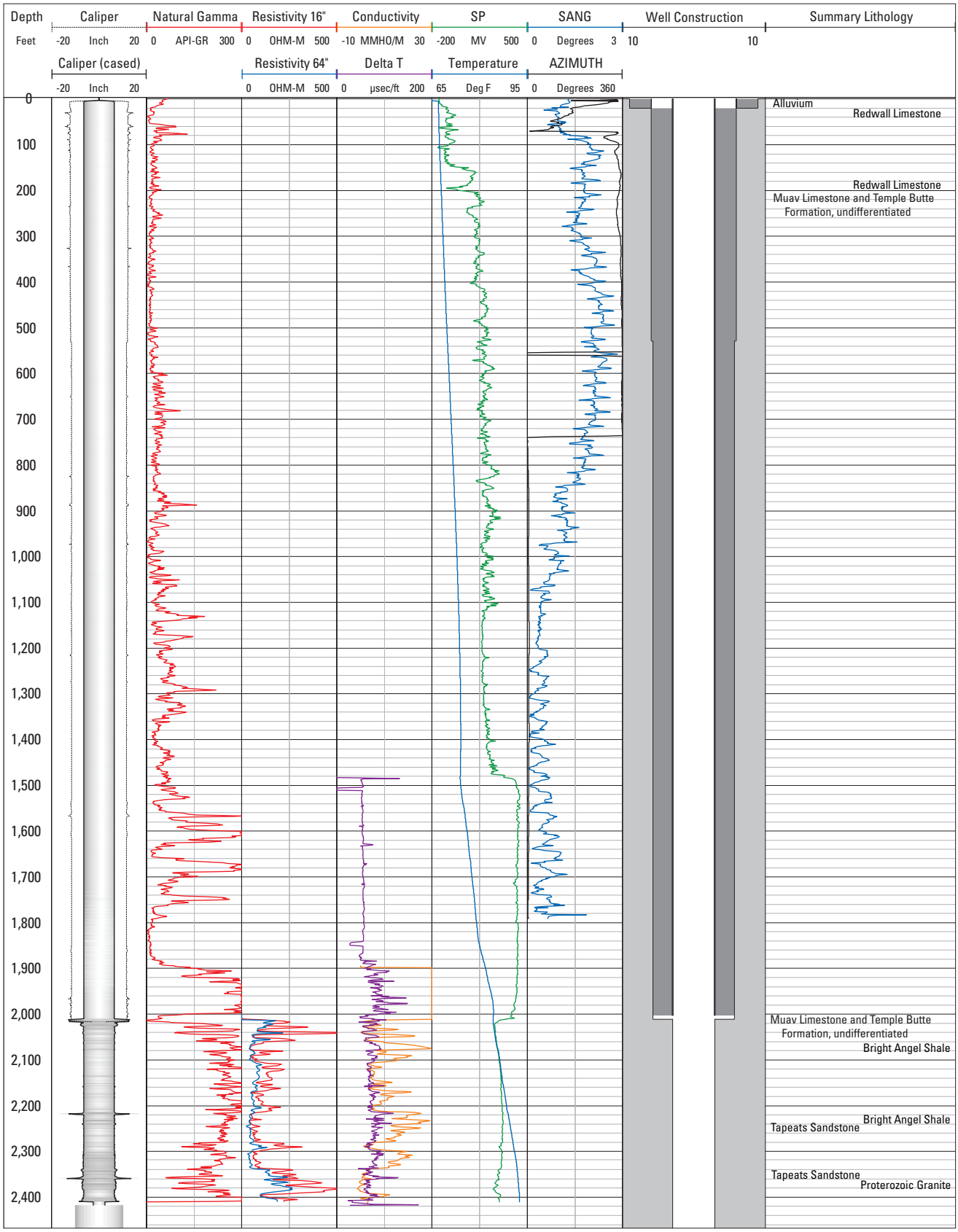

Figure 8. Plot showing the borehole logs, well construction, and summary lithology of the U.S. Geological Survey test well, western Hualapai Plateau (Hualapai Test Well on figure 1), northwestern Arizona. Ohm-meters, OHM-M; spontaneous potential, SP; millivolts, MV; delta time, Delta T; microsecond per feet, µsec/ft; degrees Fahrenheit, Deg F.

Collection of Spring and Well Data

New hydrogeologic information from spring and well inventories of the western Hualapai Plateau were collected to supplement existing data and improve the conceptual model of aquifers on the western Hualapai Plateau. There is also one streamflow-gaging station on the western Hualapai Plateau that was evaluated for the baseflow component of its record. The new hydrogeologic data included water levels from 5 wells and discharge from 31 springs with measurements of field water-quality parameters when possible (fig. 9; tables 2.1 and 2.2 of appendix 2).

Flow rate and field parameters (air temperature, water temperature, specific conductivity, pH, and dissolved oxygen) were measured at springs using a variety of methods depending on the volume of flow. Discharge from low volume springs or seeps were measured using volumetric methods. Medium volume springs were measured using a 3-inch modified Parshall Flume. Larger volume springs were measured using a pygmy flowmeter or Flowtracker Acoustic Doppler Velocimeter (ADV). About 12 of the spring sites were only accessible from the Colorado River and were measured during a river trip in May 2018. The remaining sites were measured from May 2017 to October 2018. Selected springs were measured quarterly or monthly to determine if temporal trends existed in either discharge or field parameters. Depth to water in wells was measured using a calibrated steel or electric water-level tape. Well discharge was measured for the new test well using the volumetric method. These data were used to improve the conceptual understanding of aquifers on the western Hualapai Plateau and develop a better understanding of hydraulic properties within the aquifers. Water-quality, discharge, and water-level data for the springs and wells sampled for this study are available at the USGS National Water Information System (U.S. Geological Survey, 2019).

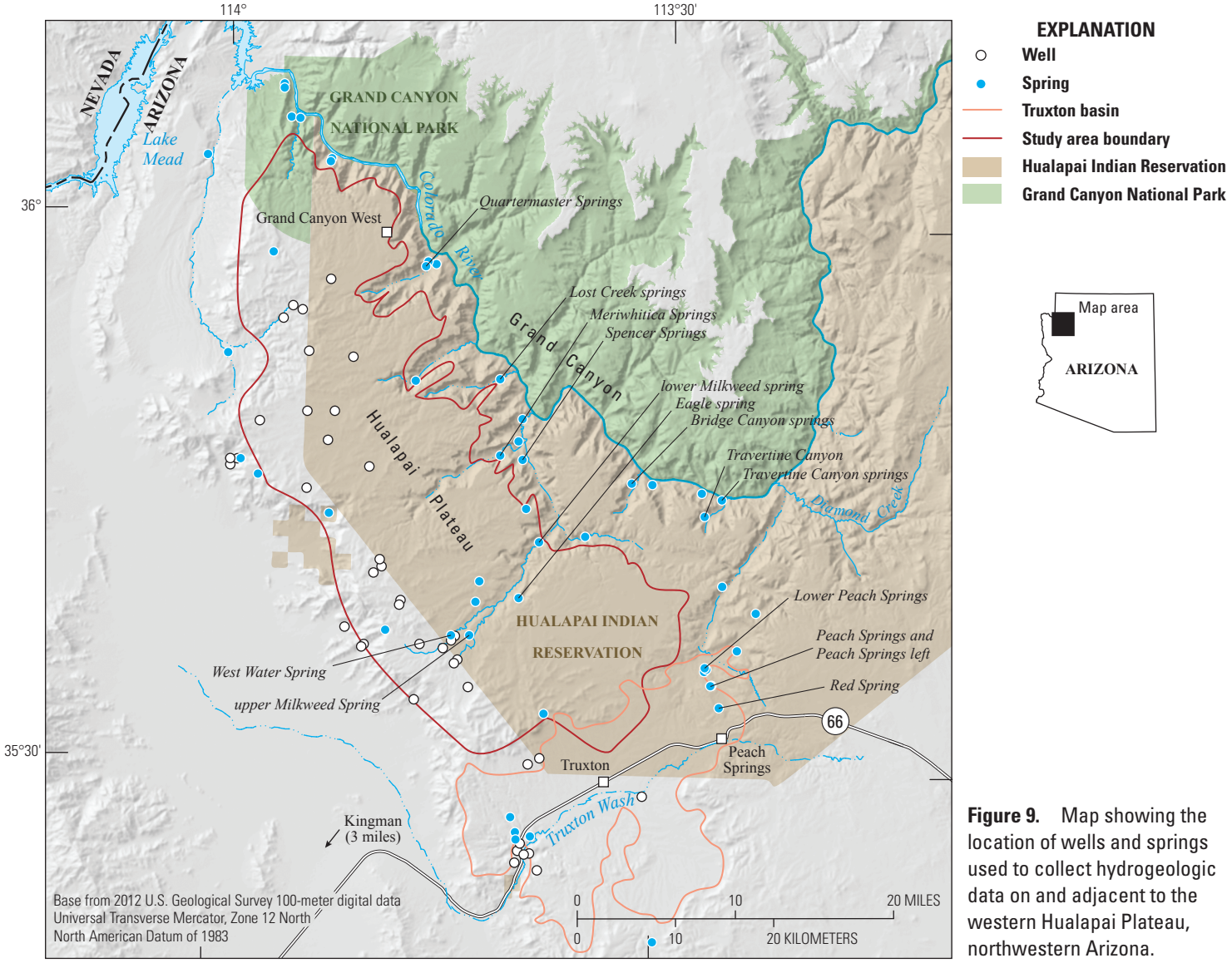

Figure 9. Map showing the location of wells and springs used to collect hydrogeologic data on and adjacent to the western Hualapai Plateau, northwestern Arizona.

Results

Evaluations of surface geophysical data were used to determine the depth to bedrock and structural features on the western Hualapai Plateau. The 2,468-ft-deep test well provided information on the subsurface lithology and resistivity of geologic units that were used to compare and provide ground-truth interpretations of the surface-based geophysical data. Other existing well, spring, geologic, and hydrologic information were used with the geophysical data to improve the understanding of both perched and bedrock aquifer characteristics on the western Hualapai Plateau.

Controlled Source Audio-Frequency Magnetotelluric Surveys

The resistivity inversions collected along nine CSAMT survey lines are discussed relative to three areas: Grand Canyon West Airport, Horse Flat, and Plain Tank Flat (figs. 1 and 7). Geologic units in these areas were combined into five stratigraphic layers that have similar electromagnetic properties. The five stratigraphic layers are listed below. All layers were not present in every survey line. The length of each CSAMT line is given in parentheses at first mention.

Layer 1—gravel deposits

Layer 2—lower Supai Group

Layer 3—Redwall Limestone, Temple Butte Formation, and Muav Limestone

Layer 4—Bright Angel Shale and Tapeats Sandstone

Layer 5—Proterozoic crystalline and metamorphic rocks

Survey near Grand Canyon West Airport

East-west CSAMT lines AP1 (5 km) and AP2 (3 km) were surveyed near the Grand Canyon West Airport (fig. 7*A*). Four stratigraphic layers are identifiable on both lines (figs. 10 and 11). The surface is a layer of moderately resistive material, about 100 to 400 ohm-meters (ohm-m; green and yellow), that corresponds to gravel deposits and the lower Supai Group (Billingsley and others, 2006). On line AP1 (fig. 10), the lower Supai Group is about 50 m thick from station 6650, thickening to about 100 m to the east at the rim of the Grand Canyon. The gravel deposits appear as slightly less resistive (green) material from about station 7050 to 7750 and again from about 8550 to about 9450, consistent with deposition on a surface eroded into the lower Supai Group. On line AP2 (fig. 11), the lower Supai Group remains about 100 m thick from west to east, and the gravel deposits are likely too thin to image.

At 100 m depth, a strong resistivity contrast exists between the gravel deposits/lower Supai Group and a more resistive layer of greater than 400 ohm-m material (red) that corresponds to the Redwall and Muav Limestones and Temple Butte Formation. On line AP1, this layer ranges from about 400 to 700 m thick from the east to the west end of the line, respectively (fig. 10). On line AP2, this layer is about 500 m thick at the west end of the line and thins to less than 100 m thick at the east end of the line. This could be caused by interference from a road with pipeline at the east end of the line (fig. 11). Below this resistive layer is a more conductive layer (200 ohm-m, green to yellow) that corresponds to Bright Angel Shale and Tapeats Sandstone. The varying thickness and vertical extent of this resistive layer is consistent with the known erosional contacts above and below the Bright Angel Shale and Tapeats Sandstone and the geologic structures intersected by the survey line. Below 500 m elevation on both lines is a strong resistor, greater than 1,000 ohm-m (red), that corresponds to Proterozoic crystalline and metamorphic rocks.

Line AP1 intersects several mapped faults and a monocline (figs. 7*A* and 10). Mapped faults that form a graben correspond with areas of relatively low resistivity in the two uppermost layers near stations 5850 and 6350 (Billingsley and others, 2006). Similarly, low resistivity values in these layers corresponds with a mapped fault near station 9100 and may indicate the presence of faults with no surface expression near stations 7250 and 8050 because they are overlain by gravel deposits. The inversion data from stations 9150 to 9750 indicate beds dipping to the east (especially in the Bright Angel Shale and Tapeats Sandstone), which correlate with a fault and monocline that occur together on geologic maps (Billingsley and others, 2006).

Line AP2 also crosses a series of mapped faults, but these faults are not very evident in the CSAMT inversion results, particularly in the Redwall and Muav Limestones, which are remarkably uniform (figs. 7*A* and 11). Near station 1750, line AP2 intersects a mapped monocline (fig. 11). The mapped monocline may account for a sharp drop off in the resistive layer representative of the Proterozoic crystalline and metamorphic rocks at the bottom of the cross section at station 1550. A road with a pipeline causes interference with the data at station 2950. The effects of this interference appear to extend westward to at least station 2350.

Survey near Quartermaster and Horse Flat Canyons

CSAMT lines QB1, QB2, and QB3 were surveyed in the area between Quartermaster and Horse Flat Canyons (figs. 1, 7*A,* and 12–14). Lines QB1 (7 km) and QB2 (6.5 km) are oriented southwest to northeast, and line QB3 (6 km) is oriented northwest to southeast (fig. 7*A*). These surveys imaged three to four identifiable stratigraphic layers on all three lines (figs. 12–14). In some areas from land surface to generally less than 50 m depth, intermittent zones of moderately resistive material (about 100 to 400 ohm-m; green and yellow) correspond to unconsolidated channel deposits and gravel deposits. In other areas, surface sediments are absent, and the Redwall Limestone is exposed, which (together with the Temple Butte Formation

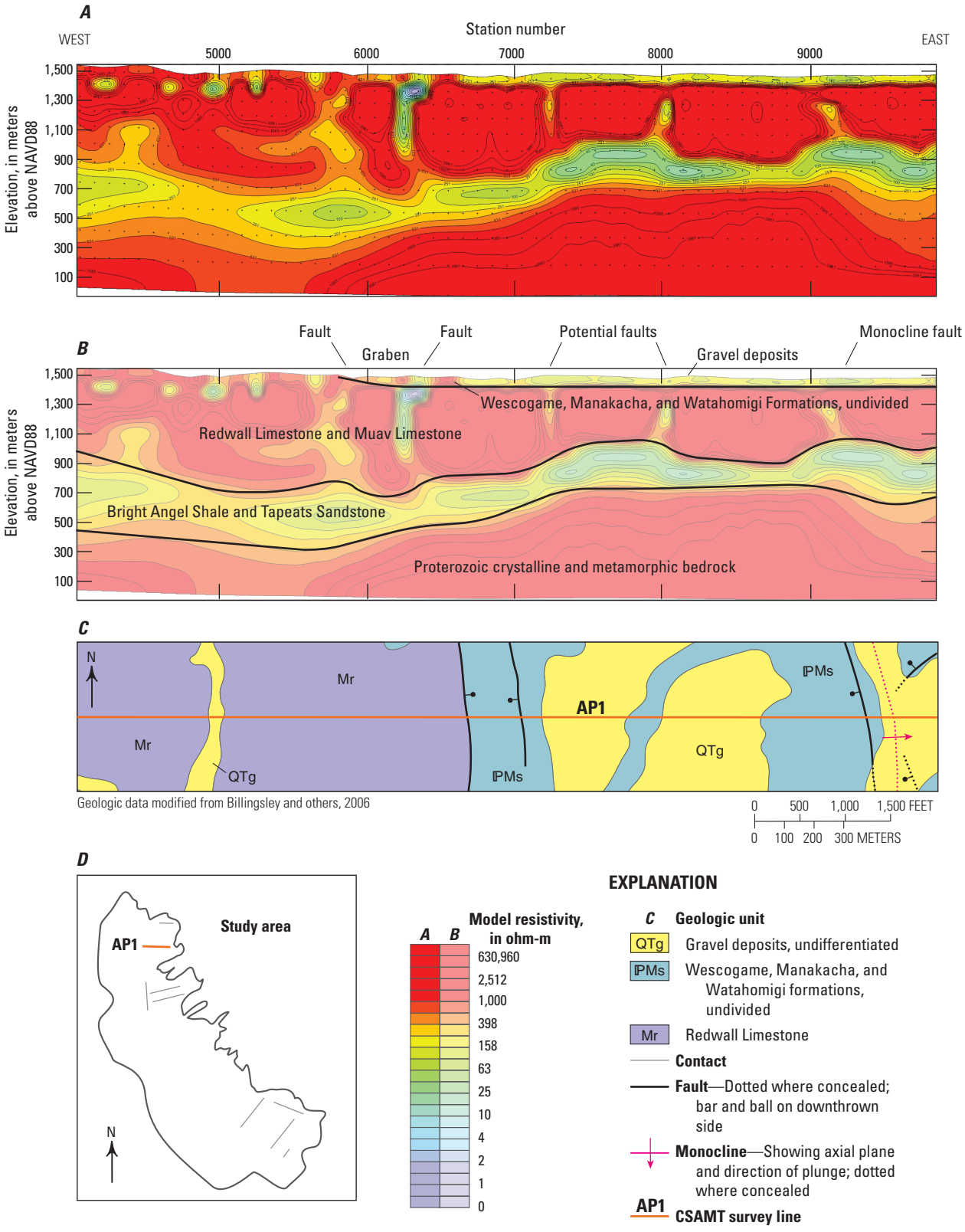

Figure 10. Diagrams showing west to east cross section of smooth model inversion results (*A*) and interpretations of inversion results for the AP1 controlled source audio-frequency magnetotelluric (CSAMT) line (*B*)h on the western Hualapai Plateau, Arizona. A separate geologic map (*C*) shows the geologic units and structure that this CSAMT line crosses.

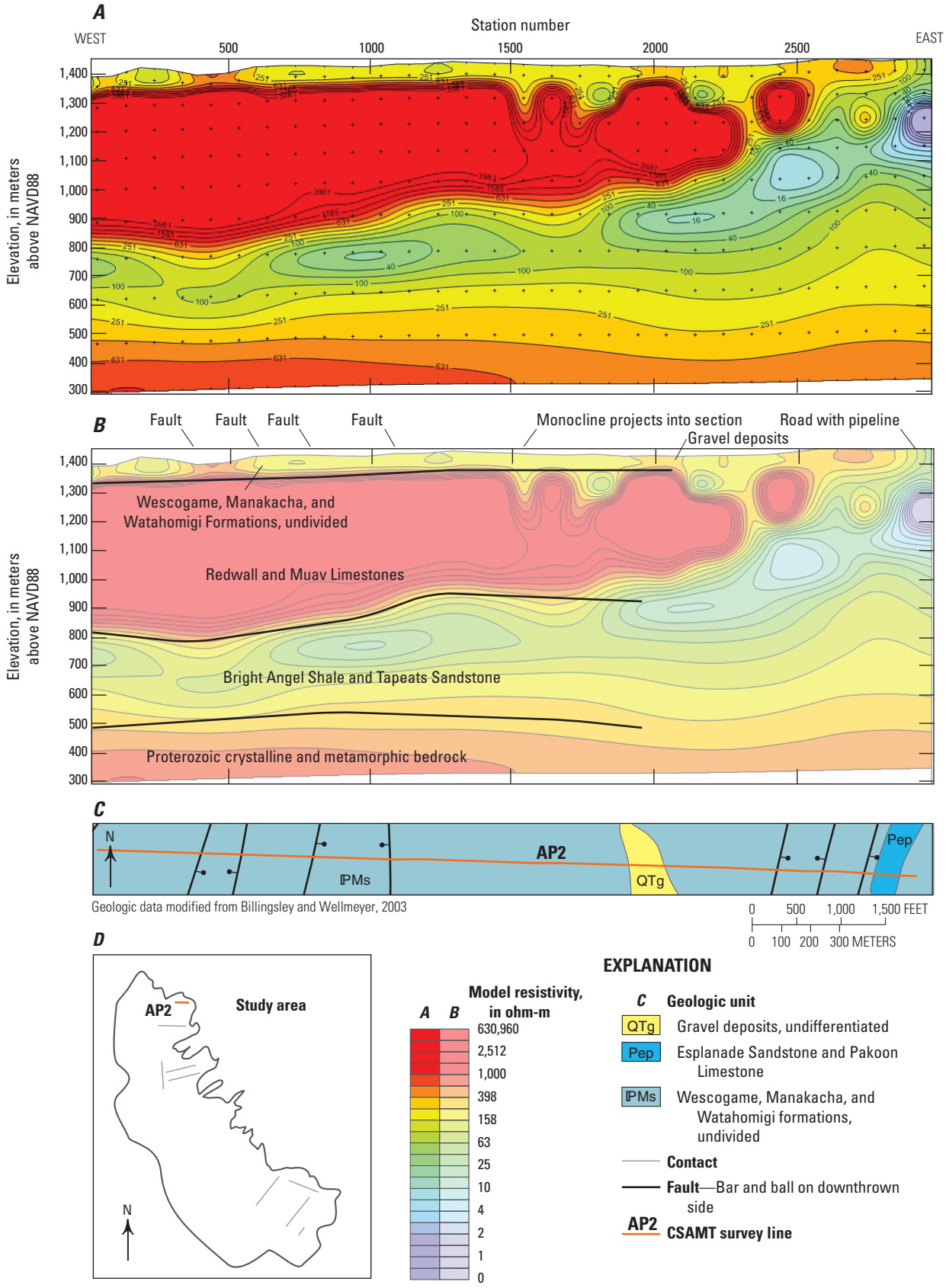

Figure 11. Diagrams showing west to east cross section of smooth model inversion results (*A*) and interpretations of inversion results for the AP2 controlled source audio-frequency magnetotelluric line (*B*) on the western Hualapai Plateau, Arizona. A separate geologic map (*C*) shows the geologic units and structure that this CSAMT line crosses.

and Muav Limestone) appears in the inversions as a more resistive layer of greater than 400 ohm-m material (red) that extends to about 1,100 m elevation. On lines QB1 and QB2 between about 1,100 to 900 and 700 m elevation, respectively, is a more conductive unit of 10 to 200 ohm-m (purple to yellow) material that corresponds to the Bright Angel Shale and Tapeats Sandstone (figs. 12, 13). Line QB3 shows the tops and bottoms of this same conductive unit to be dipping about 3° to the southeast (fig. 14). Below about 900 to 500 m elevation, the inversion data for all three lines indicate a strong resistivity of greater than 1,000 ohm-m (red) that corresponds to the Proterozoic crystalline and metamorphic rocks.

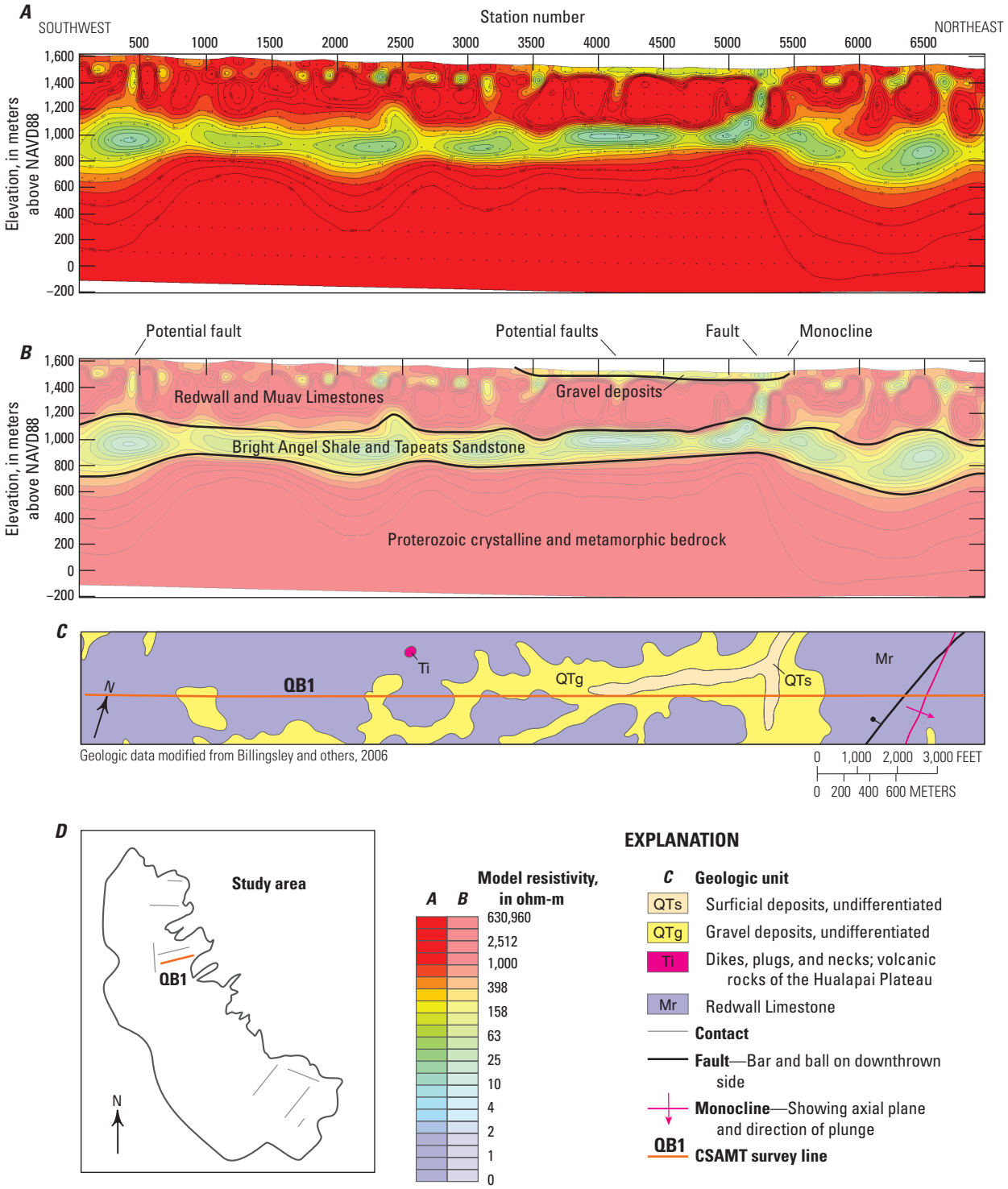

Figure 12. Diagrams showing southwest to northeast cross section of smooth model inversion results (*A*) and interpretations of inversion results for the QB1 controlled source audio-frequency magnetotelluric (CSAMT) line (*B*) on the western Hualapai Plateau, Arizona. A separate geologic map (*C*) shows the geologic units and structure that this CSAMT line crosses.

The inversion data for line QB1 indicate several high-angle faults and confirm a fault depicted on the regional geologic map (figs. 7*A* and 12, Billingsley and others, 2006). A mapped fault and monocline are located at stations 5250 and 5450, respectively. Potentially buried faults are near stations 450 and 4150. No cultural interference was indicated.

The southwest-to-northeast survey line QB2 does not transect any known or mapped faults (figs. 7*A* and 14). The resistivity profile, however, indicates several potential faults, some of which suggest significant offset of sedimentary rocks at depth. Potential high-angle faults with minimal offset are located near stations 750, 1550, and 1750. Additional, potential

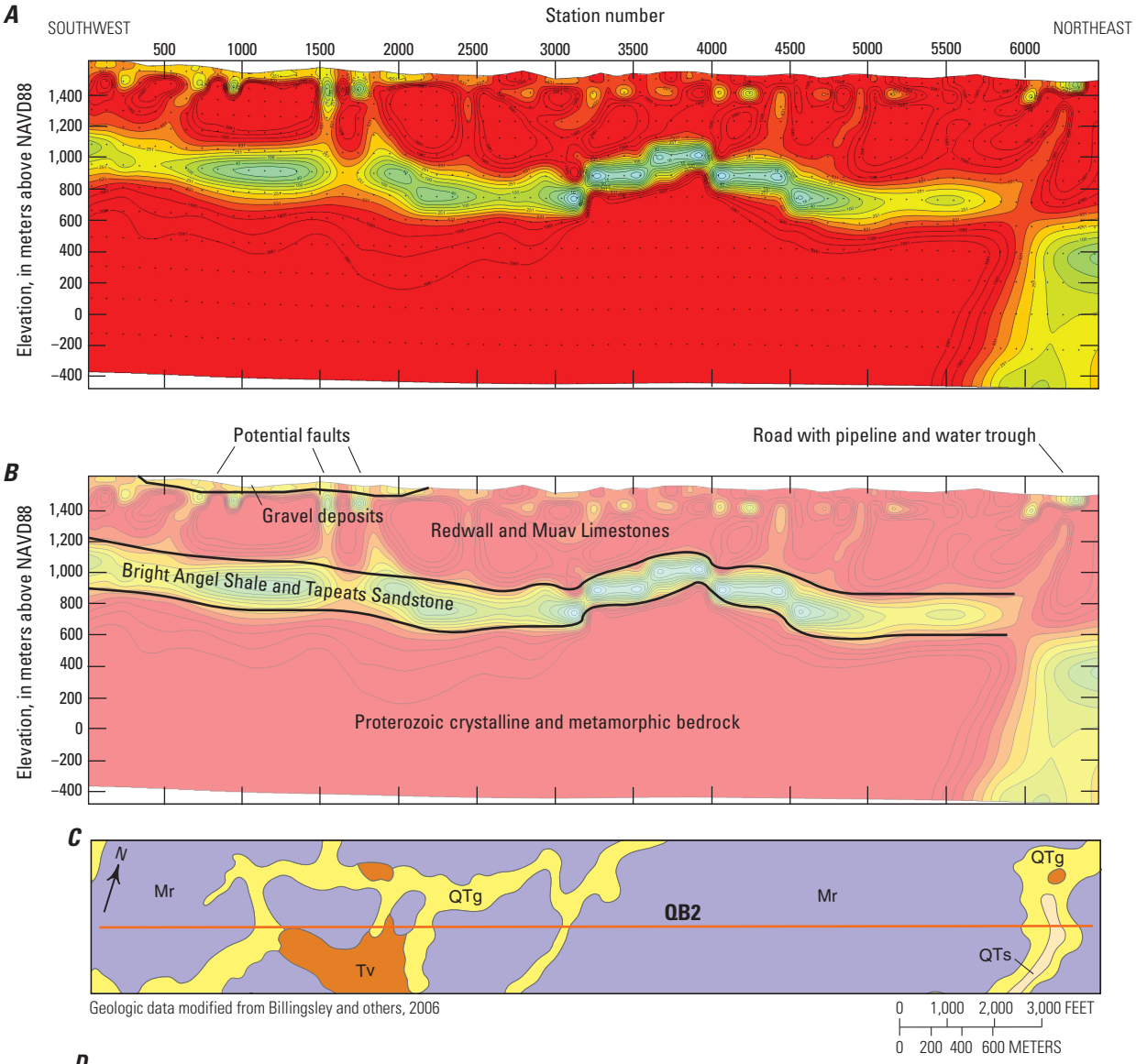

Figure 13. Diagrams showing southwest to northeast cross section of smooth model inversion results (*A*) and interpretations of inversion results for the QB2 controlled source audio-frequency magnetotelluric (CSAMT) line (*B*) on the western Hualapai Plateau, Arizona. A separate geologic map (*C*) shows the geologic units and structure that this CSAMT line crosses.

high-angle faults with apparently more significant offset are inferred at stations 3250, 4450, and 4950. Line QB2 transects a road with a water pipeline and cattle trough at station 6250, causing interference that produces an artificially conductive subsurface in the northeastern part of the survey line (fig. 13).

Survey line QB3 trends northwest to southeast (figs. 7*A* and 14) and images three stratigraphic layers. The survey line is perpendicular to several alluvial channels containing gravel deposits. Unlike survey lines QB1 and QB2, these deposits are imaged as a broken sequence of moderately resistive material,

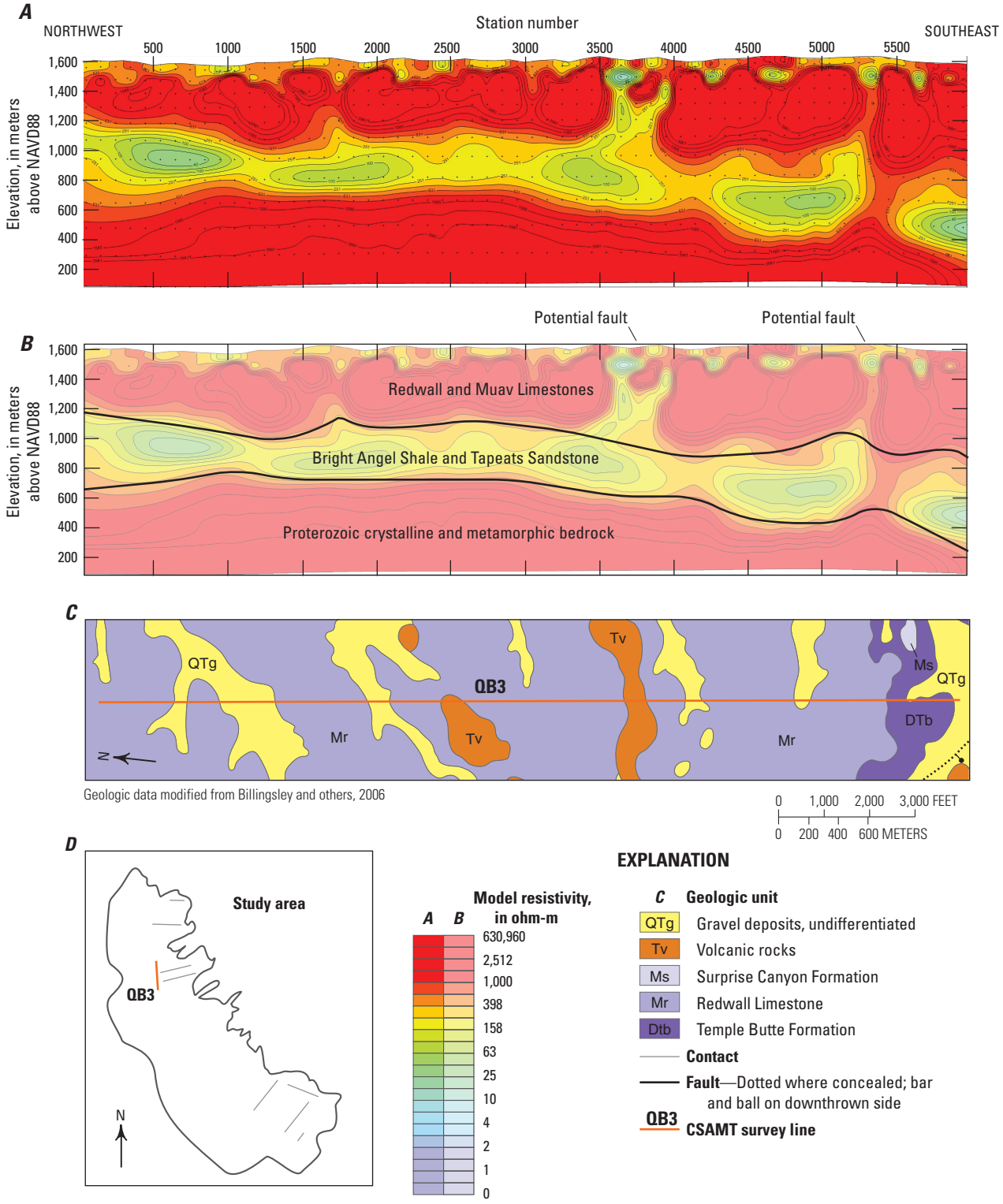

Figure 14. Diagrams showing southwest to northeast cross section of smooth model inversion results (*A*) and interpretations of inversion results for the QB3 controlled source audio-frequency magnetotelluric (CSAMT) line (*B*) on the western Hualapai Plateau, Arizona. A separate geologic map (*C*) shows the geologic units and structure that this CSAMT line crosses.

about 100 to 400 ohm-m (green and yellow) across the top of the survey line and with depths of generally less than 50 m. At station 5350, survey line QB3 appears to intersect the same mapped high-angle fault as imaged near station 5450 on survey line QB1 (figs. 12, 14). Inversion results indicate another potential fault zone at station 3750.

Survey near Plain Tank Flat

CSAMT lines PT1, PT2, PT3, and WG were surveyed in the Plain Tank Flat area (fig. 7*B*). Line PT1 is much shallower than other surveyed lines because the separation between transmitter and receiver was significantly less than other lines. Lines PT1 (8 km), PT3 (7 km), and WG (2 km) are oriented southwest to northeast, and line PT2 (8 km) is oriented southeast to northwest. Several cultural interference features in the Plain Tank Flat area include roads with water pipelines and a Federal Aviation Administration Very High Frequency, Omni-Directional Range (VOR) radio transmitter. The upper 50 to 80 m of the Plain Tank Flat area is composed of moderately resistive material of 25 to 400 ohm-m (green to yellow) that corresponds to Quaternary and Tertiary gravel and Tertiary volcanic deposits (survey lines PT1, PT2, and PT3; figs. 15–17). In survey lines PT1, PT2, and PT3, a high resistivity layer greater than 400 ohm-m (red) corresponding to the Redwall Limestone, Muav Limestone, and Temple Butte Formation is found between about 1,400 and 1,200 m elevation. In these same survey lines, a 100- to 200-m-thick resistivity layer of 10 to 200 ohm-m (purple to yellow) corresponds to Bright Angel Shale and Tapeats Sandstone and is below 1,200 m elevation. Proterozoic crystalline and metamorphic rocks underlie the Tapeats Sandstone at elevations typically below 1,000 to 800 m with resistivity values greater than 1,000 ohm-m (red).

Survey line PT1 transects several roads, all with pipelines that cause interference with the data near stations 250, 1250, 2150, 3050, 3650, 6450, 7050, and 7250 (fig. 15), which appear mostly as low-resistivity zones within the Redwall and Muav Limestone layer. Also, a VOR radio transmitter is near station 4450 on the survey line. No geologic structures are mapped on or near line PT1 (fig. 7*B*; Billingsley and others, 2006). Interference from surface roads, pipelines, and the radio transmitter make interpretation difficult for this survey line.

Survey line PT2 transects roads with pipelines at stations 2050, 2950, and 4250 that caused interference with the data (fig. 16). No apparent geologic structure is mapped on or near line PT2; however, the data suggest a ridge of Proterozoic crystalline and metamorphic rocks that rises to an elevation of about 1,200 m between stations 2850 and 3650.

Survey line PT3 transects roads with pipelines at stations 250, 550, and 5450 that cause interference with the data (fig. 17). No mapped geologic structures are transected by the survey line. Just north of the survey line from station 6950 to 7150, however, is a mapped collapse feature. The inversion data for this location indicate lower resistivity in the subsurface that could represent lateral extension of the collapse into the area of the survey line.

Survey line WG trends from the southwest to the northeast and was surveyed to better understand a possible conduit for groundwater flow from the Plain Tank Flat area to the Truxton aquifer (figs. 1, 7*B*, and 18). This area appears on the resistivity cross section as low-resistivity material in the 5 to 125 ohm-m range (blue to green) that corresponds to Quaternary and Tertiary gravel deposits. These gravel deposits are found on the southwest end of line WG from stations 150 to 750 at a range of elevation from land surface to about 1,350 m (fig. 18). Adjacent to these gravel deposits, from stations 750 to 1950, are highly resistive layers (250 to over 3,900 ohm-m; yellow orange and red) that indicate shallow occurrences of the Temple Butte Formation, Redwall Limestone, and Muav Limestone. The Temple Butte Formation is exposed at land surface and is underlain by the Muav Limestone in an area that extends from southwest of station 850 to station 1750. The Redwall Limestone is exposed at land surface farther east, near stations 1750 to 1950 (Billingsley and others, 2006; fig 7*B*). Below the Muav Limestone from about station 850 to 1850, a lower resistivity layer of 4 to 200 ohm-m correlates to the Bright Angel Shale and Tapeats Sandstone (fig. 18). Below elevations of about 1,300 m, the layer of 500 to 750 ohm-m resistivity correlates to Proterozoic crystalline and metamorphic rocks (fig. 18). Quaternary and Tertiary gravel deposits overly Proterozoic crystalline and metamorphic rocks from stations 150 to 750. This could be an area where the Paleozoic rocks were eroded, similar to the buried Paleochannels described by Young (1966, 1987).

Test Well Results

A lithologic log for the newly drilled test well was interpreted from the borehole cuttings collected in 20-ft intervals from the land surface to the bottom of the borehole at 2,468 ft below land surface (BLS). Thicknesses of the Muav Limestone, Bright Angel Shale, and Tapeats Sandstone correlate well to those determined by Billingsley and others (2006). Proterozoic granite was encountered in the borehole at 2,460 ft BLS. No water was encountered in the Rampart Cave Member (1,535 to 1,915 ft BLS) of the Muav Limestone despite several springs discharging from this unit to the south and north of the well site (Twenter, 1962; Billingsley and others, 2006; Hualapai Water Resources Program, 1999, 2004, 2009; Natural Resources Consulting Engineers, 2011). The Bright Angel Shale was also dry. Water was first encountered at about 2,400 ft BLS in the Tapeats Sandstone when water entered the

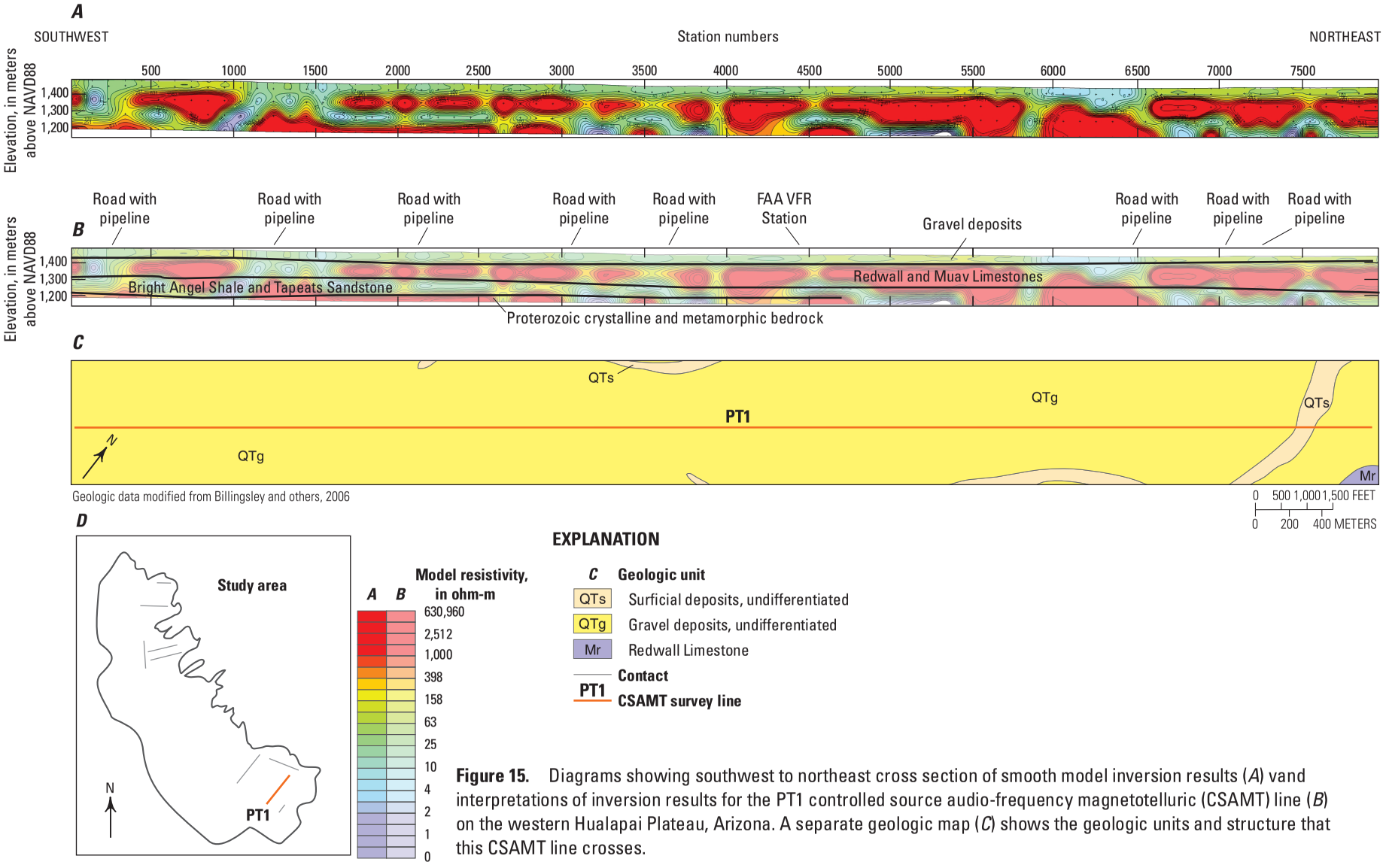

Figure 15. Diagrams showing southwest to northeast cross section of smooth model inversion results (*A*) vand interpretations of inversion results for the PT1 controlled source audio-frequency magnetotelluric (CSAMT) line (*B*) on the western Hualapai Plateau, Arizona. A separate geologic map (*C*) shows the geologic units and structure that this CSAMT line crosses.

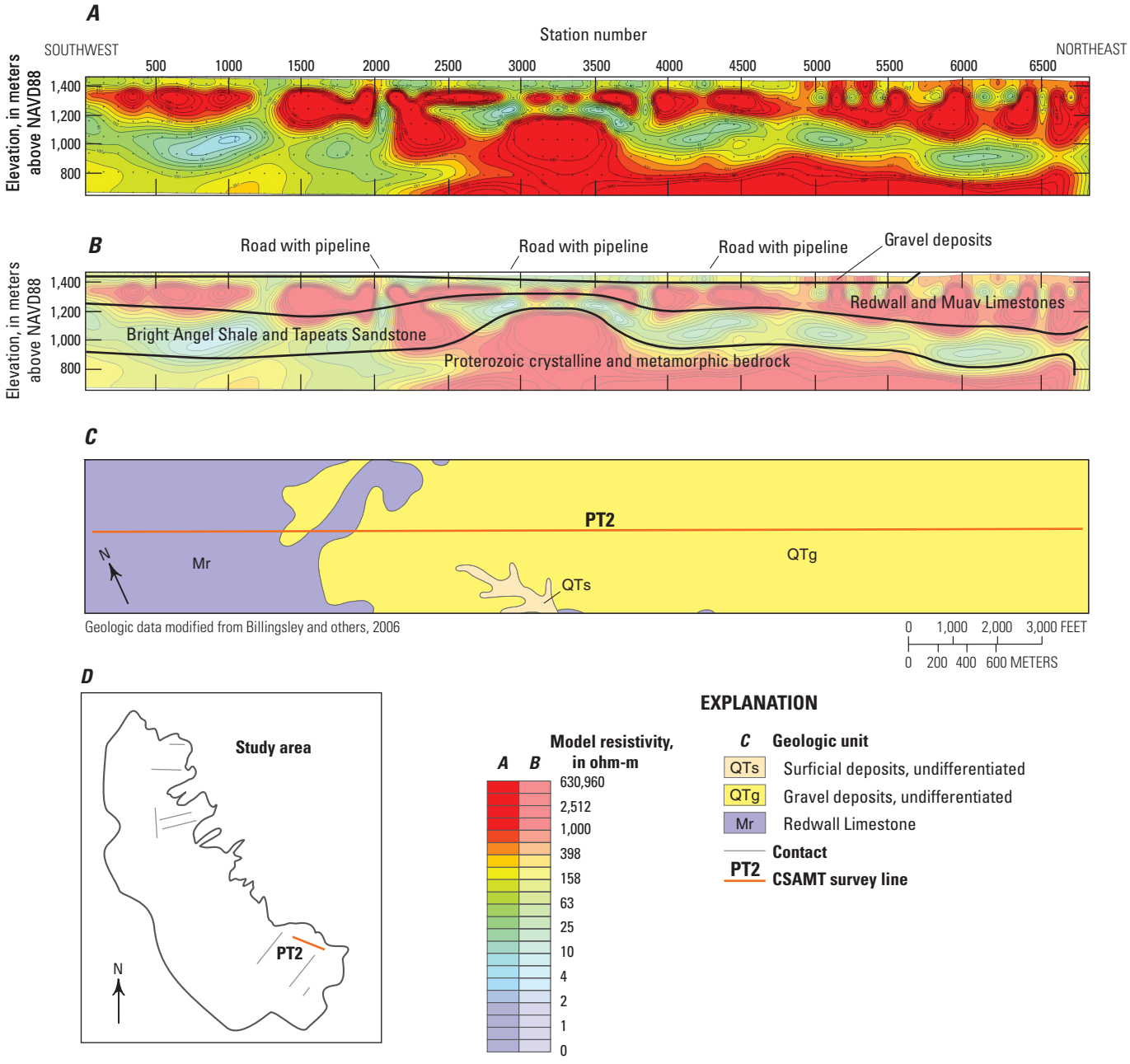

Figure 16. Diagrams showing southeast to northwest cross section of smooth model inversion results (*A*) and interpretations of inversion results for the PT2 controlled source audio-frequency magnetotelluric (CSAMT) line (*B*) on the western Hualapai Plateau, Arizona. A separate geologic map (*C*) shows the geologic units and structure that this CSAMT line crosses.

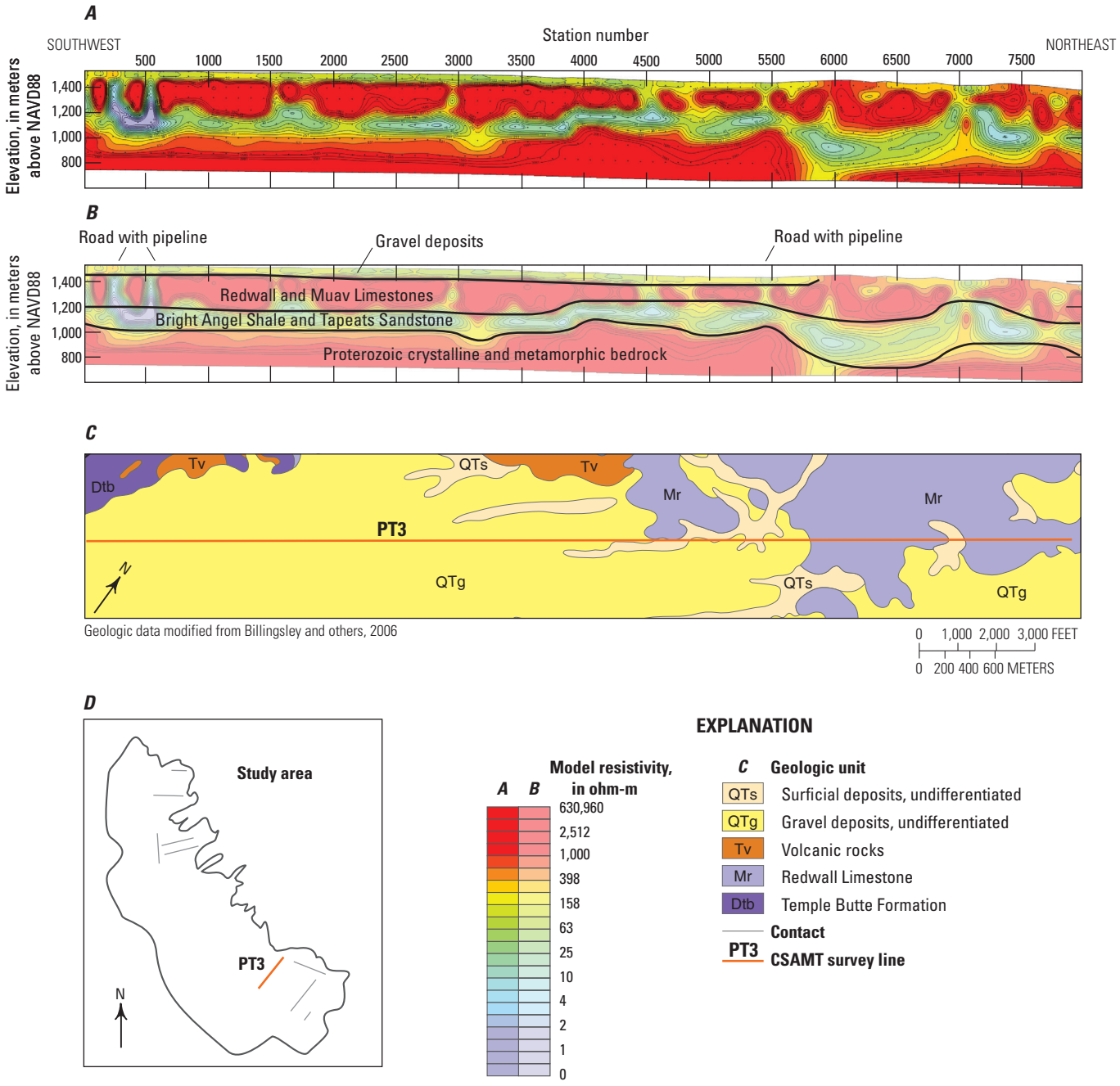

Figure 17. Diagrams showing southwest to northeast cross section of smooth model inversion results (*A*) and interpretations of inversion results for the PT3 controlled source audio-frequency magnetotelluric (CSAMT) line (*B*) on the western Hualapai Plateau, Arizona. A separate geologic map (*C*) shows the geologic units and structure that this CSAMT line crosses.

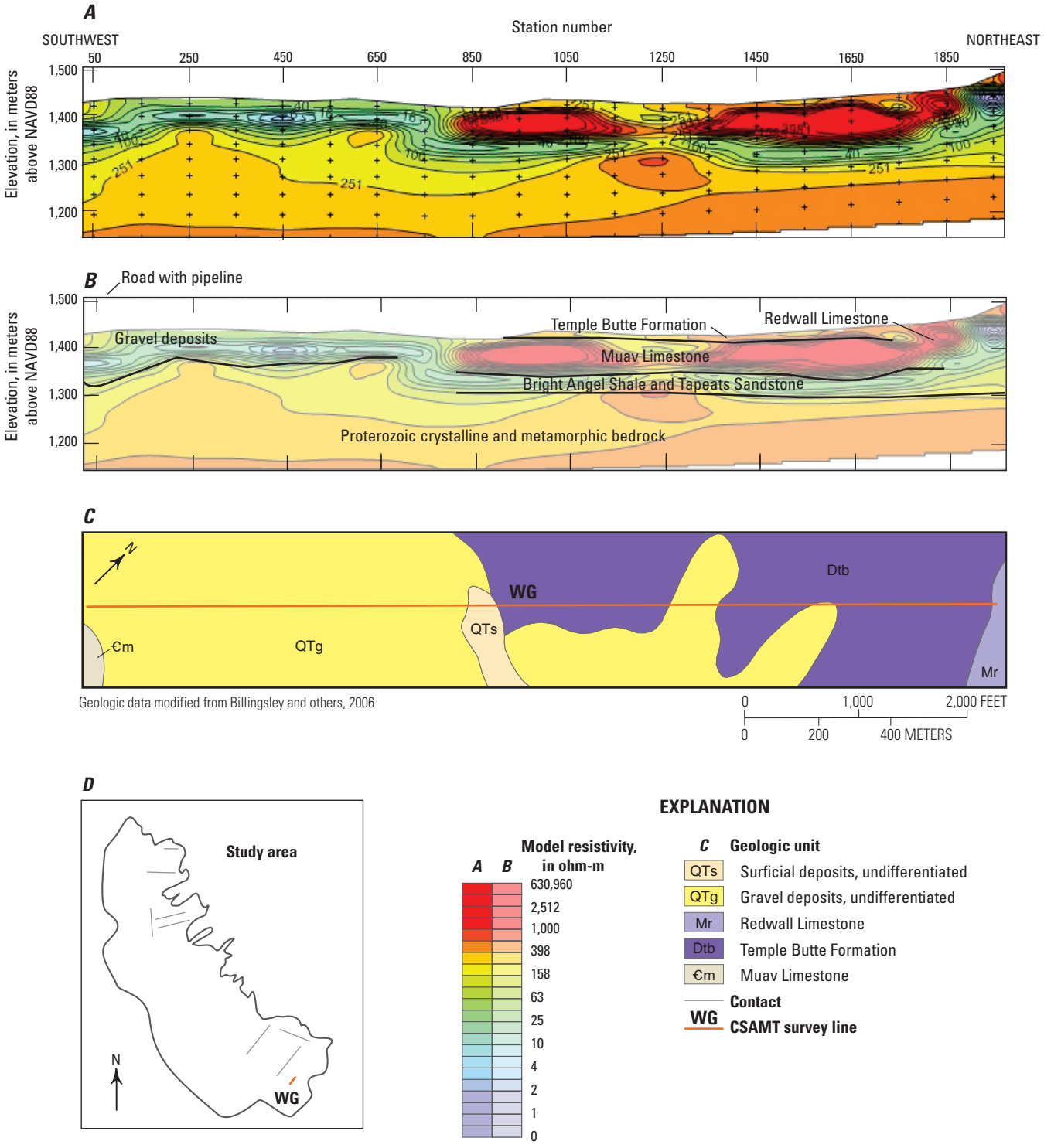

Figure 18. Diagrams showing southwest to northeast cross section of smooth model inversion results (*A*) and interpretations of inversion results for the WG controlled source audio-frequency magnetotelluric (CSAMT) line (*B*) on the western Hualapai Plateau, Arizona. A separate geologic map (*C*) shows the geologic units and structure that this CSAMT line crosses.

borehole and rose over 900 ft above the Tapeats Sandstone, which indicated it was a confined aquifer in this area. The static water level measured in the well was 1,468 ft BLS on October 17, 2018. The lithologic log for the test well indicated the thickness of the Tapeats Sandstone to only be about 60 ft.

The lithologic and borehole logs for the test well (fig. 8) were similar to those from well GCW-1, located about 8 km to the north (Watt, Bureau of Reclamation, written commun., 2000). The borehole geophysical logs of the test well correlated with the lithologic log for the test well, discussed in this paragraph from the shallowest lithology to the deepest. The gamma log remains low through the Redwall Limestone and much of the Muav Limestone. The spontaneous potential (SP) log first increases near the Muav Limestone contact (160 to 200 ft BLS), and then again at about 1,480 ft BLS. The gamma log likewise increases at about 1,560 ft BLS. The deflections in the two logs are consistent with the fine-grained (silts and mud) sediments in the Rampart Cave Member of the Muav Limestone, which is indicated in the lithologic log (table 1.1 of appendix 1). Downhole resistivity is only possible in the absence of well casing, which begins at about 2,000 ft BLS for the test well (fig. 8). The 16-inch (in.) resistivity values below the bottom of the casing at 2,000 ft BLS range from about 100 to >500 ohm-m. Resistivity from 400 to >500 ohm-m occurs at the bottom of the Muav Limestone. Resistivity 16- and 64-in. values range from about 100 to 200 ohm-m throughout the sequence of Bright Angel Shale and Tapeats Sandstone. This is consistent with resistivity values recorded by ground-based geophysical data collected to the south and north of the test-well site (figs. 7*A*, 13, and 14).

The caliper log indicated voids or open fractures just below the bottom of the casing at 2,000, 2,220, and 2,360 ft BLS. The opening at 2,000 ft BLS is interpreted as a washout from the process of cementing the casing in place. The opening at 2,220 ft BLS is close to the contact between the Bright Angel Shale and the Tapeats Sandstone, which may have been formed as the contact between lithologies widened through the circulation of water and foam in the borehole. A problem with the drill bit at about 2,360 ft BLS led to water being added to the circulating air, which may have removed unconsolidated material from the borehole in this area. The drill bit was replaced after a depth of about 2,380 ft BLS was reached.

The Papadopulos and Cooper solution for nonleaky confined aquifers (Papadopulos and Cooper, 1967) was chosen for analyzing the pumping test data. This method for analyzing single-well pumping tests includes a correction for well bore storage and was used to analyze both drawdown and recovery data (fig. 19). The estimated transmissivity and storativity values calculated from this method were 4.7 foot squared per day (ft^2/d) and 2.1 x 10^{-4}, respectively. Hydraulic conductivity, estimated as transmissivity divided by the saturated thickness (60 ft), is about 7.8 x 10^{-2} foot per day (ft/d). The estimated transmissivity values are in the range of values reported for fine to medium well-cemented sandstones (Freeze and Cherry, 1979). The drawdown and recovery data indicate that the water-bearing zone in the confined Tapeats Sandstone is relatively non-transmissive and not expected to yield large amounts of water to wells. The estimated specific capacity of the well is about 0.022 gallon per minute per foot [(gal/min)/ft] of drawdown, as calculated with the pumping rate of 4.5 gal/min and total drawdown of 205 ft. This test well and GCW-1 are the only bedrock wells where pumping tests have been conducted on the western Hualapai Plateau. Additional wells on the western Hualapai Plateau are needed to develop a better understanding of aquifer properties of the Muav aquifer across varied geologic conditions and to better understand the

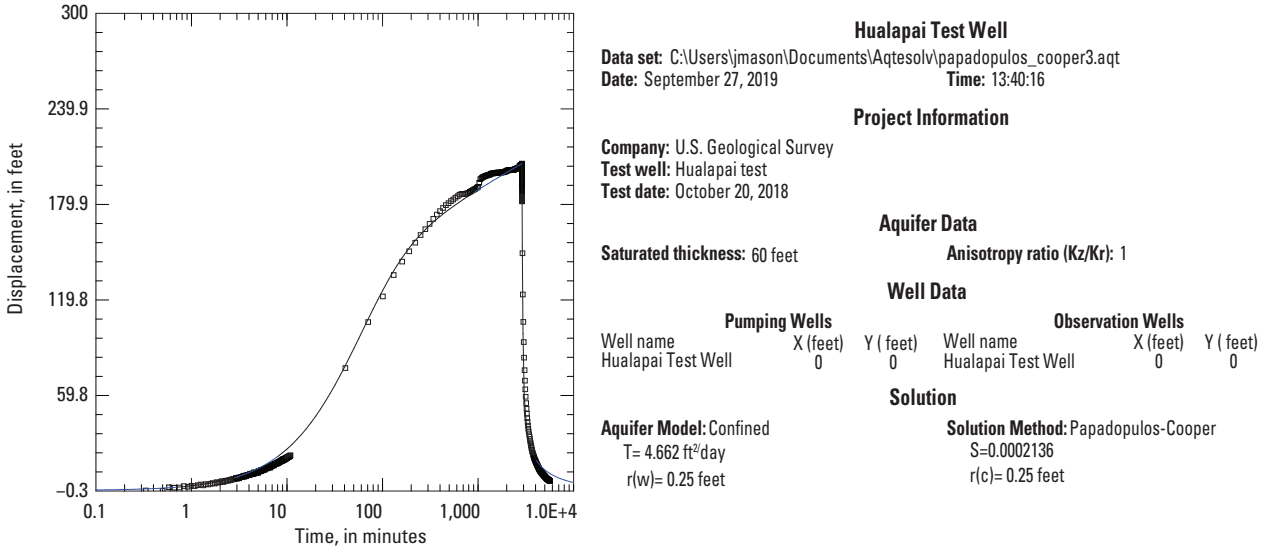

Figure 19. Graph and table showing estimated aquifer properties using the Papadopulos and Cooper solution for nonleaky confined aquifers for U.S. Geological Survey Hualapai Test Well on the western Hualapai Plateau, Arizona (Papadopulos and Cooper, 1967); ft^2/day refers to foot squared per day.

relation of confined groundwater in the Tapeats Sandstone to the Muav aquifer.

Temperature, specific conductance, pH, and dissolved oxygen were monitored by a multiparameter probe in a flow-thru chamber during the pumping test using standard USGS protocols (U.S. Geological Survey, variously dated). The flow-thru chamber was fed by a pipe plumbed into the side of the well discharge pipe. During the pumping test, discharge of about 4.5 gal/min was maintained, with about 0.1 gal/min of the total discharge flowing through the flow-thru chamber.

The pump intake was set at about 1,820 ft BLS and plumbed to the surface with a 2-inch steel pipe. At a discharge of 4.5 gal/min, it took about 1 hour for water to travel from the pump intake to the flow-thru chamber. Total purge time for one well volume of water was about 5 hours. The pump was only tested for a few minutes after it was installed prior to the 48-hour pumping test. The well was drilled using water from Lake Mead, so the initial water pumped from the well was partially from that source, and parameters were initially affected by these residual drilling fluids in the well. Water temperature measured in the flow-thru chamber also was affected by the time it took water to go from the pump intake to the flow-thru chamber. Water temperature was about 35 °C at the pump intake (based on temperatures from transducer and borehole log) but was lower during the hour it took to reach the flow-thru chamber. In addition, flow to the flow-thru chamber was not always constant and had to be adjusted at times. This further affected the water-quality parameters measured in the flow-thru chamber. Sudden fluctuations in the data in figures 21*A* through 21*D* at approximately 1,650 minutes are thought to be related to an increase in flow into the flow-thru chamber and not related to well-water characteristics.

Water temperature was 17.4 °C at the beginning of the pumping period and 18.8 °C at the end, with mid-pumping values ranging from 16.1 to 26.8 °C. A plot of the water temperature data (fig. 20*A*) shows that the temperature rose steadily from the beginning of the pumping test until about 1,000 minutes (24.5 °C) at which time it began to slowly drop. At about 1,650 minutes, the temperature increased rapidly to around 26 °C when flow to the flow-thru chamber was increased. The temperature peaked to 26.8 °C at 2,000 minutes and then began to slowly decrease again until the end of the test, likely because of a gradual decrease in flow to the flow-thru chamber.

Specific conductance (an indication of the concentration of total dissolved solids in the water) ranged from 503 to 710 microsiemens per centimeter (µS/cm) during the pumping test (fig. 20*B*). The specific conductance was 522 µS/cm at the start of the pumping test and rose steadily to 710 µS/cm at about 600 minutes into the test as water in the casing was replaced by formation water. From about 600 minutes to the end of the pumping test, specific conductance slightly declined to 677 µS/cm. A 10 µS/cm spike in the specific conductance occurred at about 1,650 minutes and was likely caused by changes in the flow rate to the flow-thru chamber (fig. 20*B* and 20*E*).

The pH of well water was 9.1 at the beginning of the pumping test and decreased steadily as water in the casing was replaced by formation water (fig. 20*C*). After about 2,000 minutes, the pH stabilized at 7.3 and remained relatively constant for the remainder of the test.

During the pumping test, dissolved oxygen (DO) ranged from 0 to 0.51 mg/L (fig. 20*D*). Measured DO was 0.39 mg/L at the start of pumping and dropped rapidly to 0 within the first 60 minutes of the test. After the first 60 minutes, measured DO continued to generally rise, with some decreases of DO, for the remainder of the pumping period. Final DO was measured to be 0.49 mg/L. The DO seemed to be most sensitive to changes in the flow volume in the flow-thru chamber (fig. 20*D* and 20*E*). DO values were very close to 0 for the duration of the pumping period as could be expected from a deep, confined aquifer.

Near the end of the pumping test, a water-quality sample was collected and analyzed for major ions, trace metals, nutrients, stable isotopes, and radionuclides. The sample was a calcium, magnesium-bicarbonate water type with a total dissolved-solids concentration of 371 mg/L. Alpha radioactivity of the water-quality sample was 18.3 picocuries per liter (pCi/L), which exceeds the U.S. Environmental Protection Agency (EPA) maximum contaminant level (MCL) of 15 pCi/L for drinking water (U.S. Environmental Protection Agency, 2003). In addition, concentrations of iron and manganese in the water sample exceeded the EPA secondary maximum contaminant levels (SMCL) for drinking water of 300 micrograms per liter (µg/L) and 50 µg/L, respectively. Notably, the iron concentration of the water sample was more than 10 times higher than the SMCL. Complete water-quality results for this sample are presented in table 1.3 of appendix 1.

Spring and Well Data Results

Spring-water discharge (flow) and water-quality parameters from 56 springs on and adjacent to the western Hualapai Plateau were compiled for this study, and new discharge measurements and water-quality data were collected from 31 springs. Discharge from the 31 springs visited as part of this study ranged from dry to about 345 gal/min, whereas historical spring discharge measurements ranged up to 7,540 gal/min. Discharge from springs that issued from basin-fill sediments ranged from dry to 20.2 gal/min. Discharge from springs that issued from the Muav aquifer ranged from 1 to about 345 gal/min. Discharges ranged from dry to 9 gal/min at the few springs visited issuing solely from Proterozoic crystalline and metamorphic rocks. Springs issuing from the Tapeats Sandstone were not visited as part of this study, but available historical measurements from the Tapeats Sandstone are as much as 90 gal/min.

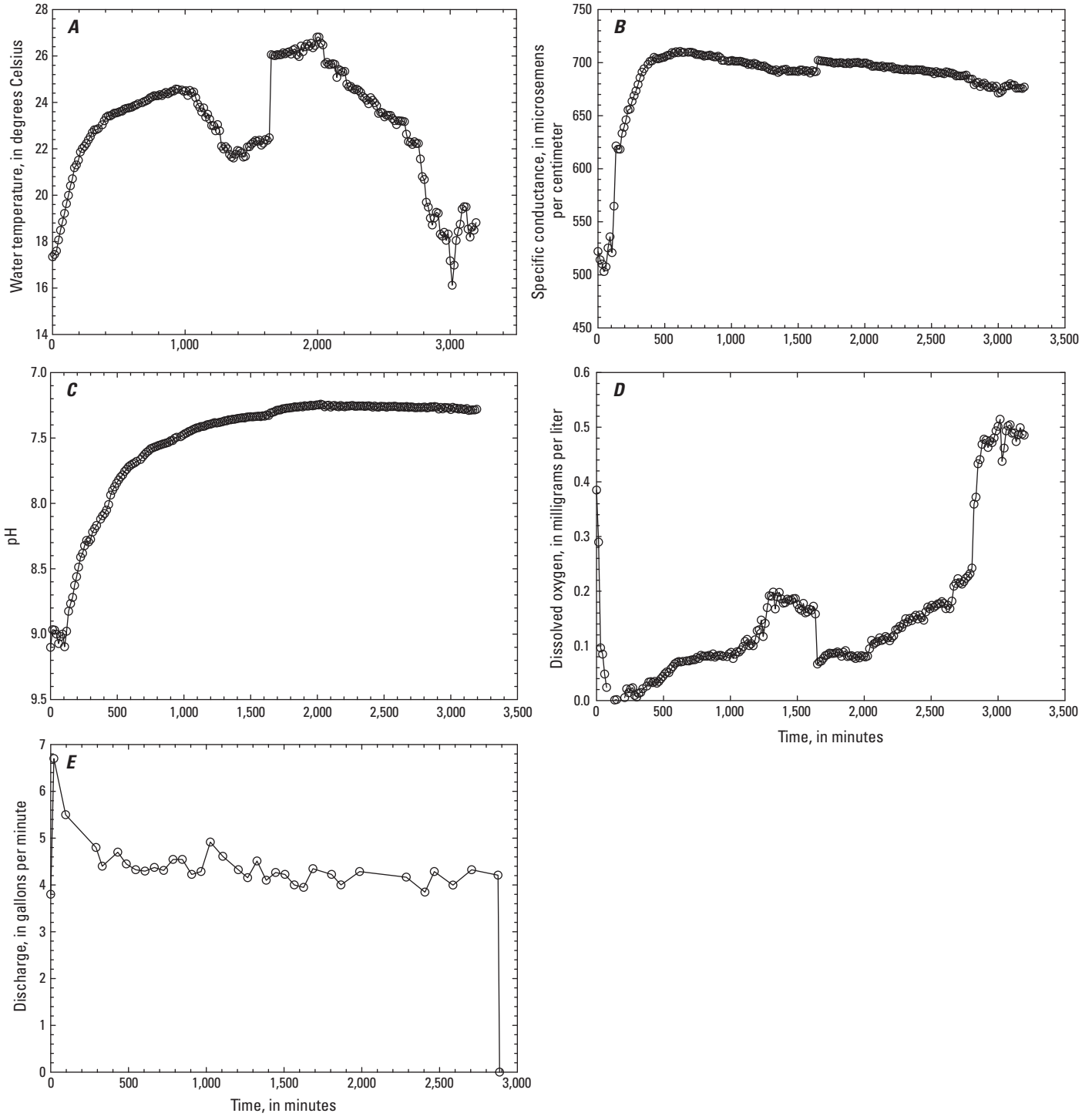

Figure 20. Graphs showing water temperature (*A*), specific conductance (*B*), pH (*C*), dissolved oxygen (*D*), and discharge (*E*) from the U.S. Geological Survey Hualapai Test Well during the 48-hour pumping test, western Hualapai Plateau, Arizona.

The water-quality field parameters for the springs visited on the western Hualapai Plateau and historical field parameters are shown in table 2.1 of appendix 2. Only field parameters collected as part of this study are discussed in the following paragraph.

In general, the water quality of springs issuing from basin-fill sediments was acceptable for most public supply, domestic, and livestock uses, where specific conductance values ranged from 583 to 905 µS/cm, pH values ranged from 7.2 to 8.3, and DO values ranged from 2.5 to 8.6 mg/L. The water quality of springs that issue from the Muav aquifer also was acceptable for most public supply, domestic, and livestock uses. The specific conductance of spring water issuing from the Muav aquifer ranged from 554 to 945 µS/cm. The higher specific conductance values are likely the result of the groundwater being in contact with limestone that easily dissolves in water. For springs that discharge from the Muav aquifer, the pH and DO ranged from 7.7 to 8.8 and 4.1 to 9.0 mg/L, respectively. Field parameters were not collected from any springs issuing from the Tapeats Sandstone as part of this study, although historical water-quality parameters were available from one Tapeats Sandstone spring (table 2.1 of appendix 2). Water quality was suitable for livestock use, but marginal for public supply or domestic uses, based on a specific conductance value of 1,680 µS/cm. Water-quality field parameters were only collected from one spring issuing exclusively from Proterozoic crystalline and metamorphic rocks. The water quality was acceptable for most public supply, domestic, and livestock uses. The spring water had a specific conductance of 755 µS/cm and a pH of 7.5.

Spring discharge on the western Hualapai Plateau is highly variable and likely dependent on the seasonal and annual availability of precipitation that supports recharge. In the 1990s, several repeat measurements of discharge were made under both wet and dry conditions. Spring discharge was measured at several of the principal springs that issue from the Muav aquifer (Travertine Canyon spring, Travertine Canyon above the mouth, Bridge Canyon spring, Eagle spring, lower Milkweed Spring, Meriwhitica Springs, Lost Creek spring, and Quartermaster Springs; fig. 9). Travertine Canyon above the mouth and Lost Creek spring also were measured in 2018. Measured discharge during dry and wet conditions ranged over several orders of magnitude (table 1).

This study also compared seasonal measurements at six springs as an indication of seasonal trends. Four of the six springs issue from basin-fill sediments (West Water Spring, upper Milkweed Spring, Red Spring, and Peach Spring left; fig. 9; table 2). The two remaining springs, Peach Springs and Lower Peach Springs, issue from the Muav Limestone. For all six springs, discharge was relatively high in the winter and then declined through the spring and summer when the effects of evapotranspiration are less and greater, respectively.

Winter discharge of Spencer creek, when evapotranspiration is lowest and storm runoff is minimal, is a further indication of groundwater flow. The USGS streamflow-gaging station at Spencer creek (09404222) is just downstream of both Spencer Springs and Meriwhitica Springs and therefore represents a composite discharge of these two springs. Median winter discharge (November 1–February 28 of each water year) of Spencer creek for the period of record (1999 to 2018) was used to evaluate the magnitude of baseflow from groundwater (fig. 5). The median discharge was used since it is less affected by occasional winter precipitation runoff events than the mean discharge. The average value of the 20 yearly median winter discharges is 3.3 ft^3/s (about 1,500 gal/min). This is not an actual measurement of baseflow, but it serves as a reference for the approximate magnitude of what baseflow likely was during that period.

Water levels from 36 wells on and adjacent to the western Hualapai Plateau were compiled for this study, and new water levels were collected from 4 wells. The new water levels are compared to historical measurements from the same wells in table 3. Water levels from the Bureau of Land Management, Horse Flat well 2 showed little change. Water levels in the Upper Milkweed 1 and Cedar Springs 1 wells were lower than the historical levels. The water level from an unnamed well (USGS 352831113303901) had a higher water level in 2018 compared to the historical measurements available.

Table 1. Discharge measurements from springs issuing from the Muav Limestone, western Hualapai Plateau, Arizona.

[E, estimated value; gal/min, gallons per minute]

U.S. Geological Survey identification number	Date measured	Discharge, in gal/min
Travertine Canyon spring		
354406113263400	May 15, 1993	552
	June 6, 1994	898
	December 8, 1994	821
Travertine Canyon above the mouth		
354503113252600	August 22, 1991	256
	August 6, 1992	346
	May 15, 1993	615
	June 6, 1994	848
	December 8, 1994	1,070
	May 21, 2018	345
Bridge Canyon spring		
354550113313400	August 6, 1992	45
	May 15, 1993	215
	June 9, 1994	27
	December 8, 1994	40
Eagle spring		
353921113390200	August 6, 1992	5 E
	May 18, 1993	1,023
	June 8, 1994	Dry
lower Milkweed Spring		
354228113374300	August 6, 1992	5 E
	May 16, 1993	22
	June 8, 1994	157
	December 8, 1994	121
Meriwhitica Springs		
354711113403200	May 16, 1993	7,315
	June 7, 1994	1,230
Lost Creek spring		
355124113404000	May 17, 1993	3,568
	June 7, 1994	260
	December 6, 1994	94
	May 22, 2018	40
Quartermaster Springs		
355748113454500	August 25, 1991	189
	May 17, 1993	7,540
	June 10, 1994	2,290
	December 7, 1994	1,795

Table 2. Seasonal variability of spring discharge measurements from six springs on the western Hualapai Plateau, northwestern Arizona.

[USGS, U.S. Geological Survey; 122SDMR, Holocene to Paleocene sedimentary and volcanic rock; 374MUAV, Cambrian Muav Limestone; gal/min, gallons per minute; E, estimated value; date measured is in month, day, year format]

U.S. Geological Survey identification number	Common spring name	Aquifer code	Flow measurements, in gal/min							
			Winter	Date measured	Spring	Date measured	Summer	Date measured	Fall	Date measured
353710113433200	West Water Spring	122SDMR	0.74	01/17/17	Dry	05/10/18	Dry	06/19/18		
353713113421800	Upper Milkweed	122SDMR	20.2	01/17/17	9.4	05/10/18				
353333113251801	Red Spring	122SDMR	0.72	02/14/18			0.25E	06/13/18		
							0.1E	08/30/18		
353444113255401	Peach Spring Left	122SDMR	15.7	01/17/18	13.5	03/07/18	5.16	06/05/18	4.49	10/04/18
					8.98	04/16/18	9.87	08/08/18		
353532113262101	Lower Peach Spring	374MUAV	2.2	01/17/18	1.6	03/14/18	0.01	08/30/18		
					1.4	04/24/18	Dry	09/11/18		
353445113255000	Peach Spring	374MUAV/ 122SDMR	76	01/17/18	62.8	03/07/18	61.9	06/05/18	58.3	10/04/18
					67.3	04/16/18	63.3	08/08/18		

Table 3. Comparison of water levels from wells measured in 2018 with historical water-level measurements, western Hualapai Plateau, Arizona.

U.S. Geological Survey identification number	Common well name	Aquifer code	Depth of well, in feet BLSD	Depth to water, in feet BLSD	Date measured
354918113535701	BLM, Horse Flat Well 2	122SDMR	--	82.50	6/14/84
				87.70	4/22/87
				83.40	11/8/95
				84.01	5/22/18
354615113590901	Cedar Spring Well 1	400GRNT	175	70.10	3/25/80
				79.50	12/4/85
				80	1/1/86
				73.10	11/8/95
				108.9	2/8/18
353538113433101	Upper Milkweed Well 1	122SDMR	35	14.80	6/14/84
				15.30	4/22/87
				9.40	11/8/95
				25.38	6/19/18
352831113303901	unnamed	---	100	69.10	4/23/80
				62	12/6/85
				62	1/1/86
				61.60	4/23/87
				61.80	10/16/92
				54.20	9/4/18

Summary

This study used ground-based geophysical surveys and combined new and existing well, spring, and other hydrogeologic information available from previous studies to develop a better understanding of the hydrogeology of the western Hualapai Plateau. Data were also collected for future use in a numerical groundwater model for the Hualapai Indian Reservation.

Geophysical methods were used to develop a better understanding of the geologic framework of the western Hualapai Plateau groundwater-flow systems. The surface geophysical method, controlled source audio-frequency magnetotellurics (CSAMT), penetrated to the Proterozoic crystalline and metamorphic rocks that underlie the western Hualapai Indian Reservation, providing a good control on the lower limit of groundwater flow. Three sets of CSAMT survey lines were collected: one at the Grand Canyon West Development, one between Quartermaster Canyon and Horse Flat Canyon, and one in the Plain Tank Flat area. Although the CSAMT surveys in the Grand Canyon West area identified several deep geologic structures, this area was not pursued for further exploration because of the lack of groundwater discharge from springs in tributary canyons. The CSAMT survey in the area of Quartermaster and Horse Flat Canyons identified a few previously unknown deep structural trends that may be faults with the potential to act as conduits for groundwater flow. Springs discharge significant, if variable, amounts of groundwater from the Rampart Cave Member of the Muav Limestone in both Quartermaster and Horse Flat Canyons. For this reason, a site was selected in this region for drilling a test well.

The Hualapai Test Well (referred to as the test well) between Quartermaster and Horse Flat Canyons was drilled to obtain additional information about the geophysical properties of geologic formations at depth. The data were used as an independent means of verifying the results of surface geophysical data and to evaluate groundwater-development potential if sufficient water was present in the test well. The test well was drilled to a depth of 2,468 feet (ft) with the bottom 8 ft in Proterozoic granite. Borehole geophysical logs collected from the test well provided resistivity 16-inch values for the different geologic formations encountered that correlate with the resistivities determined from the CSAMT surveys. The Muav Limestone, where water was expected, was dry as was the Bright Angel Shale. Water was first encountered in the test well at a depth of 2,400 ft in the Tapeats Sandstone. At the test well site, the Tapeats Sandstone is confined and had a hydrostatic head of over 900 ft, which caused the static water level in the test well to rise to an elevation of 1,468 ft.

A 48-hour pumping test with an additional 48 hours of monitored recovery was conducted at the test well. The discharge rate was 4.5 gallons per minute (gal/min) during the pumping test, which resulted in a maximum drawdown of about 205 ft recorded with a pressure transducer. Data for recovery were recorded until the water level reached 97 percent of the pre-drawdown level. The Papadopulos and Cooper solution for nonleaky confined aquifers (Papadopulos and Cooper, 1967) was used to estimate aquifer parameters. The estimated transmissivity was 4.7 square feet per day. The estimated storativity was 2.1×10^{-4}, the hydraulic conductivity was about 7.8×10^{-2} foot per day, and the estimated specific capacity of the test well is about 0.022 gallon per minute per foot of drawdown. The hydraulic properties for the test well indicated that although groundwater is present in the Tapeats Sandstone, yields are likely to be small.

A water-quality sample was collected from the test well, and analyses indicated the sample had a calcium, magnesium-bicarbonate water type with a total dissolved-solids concentration of 371 milligrams per liter (mg/L). Alpha radioactivity of the sample was 18.3 picocuries per liter (pCi/L), which exceeded the U.S. Environmental Protection Agency (EPA) maximum contaminant level of 15 pCi/L for drinking water. Concentrations of iron and manganese in the water sample also exceeded the EPA secondary maximum contaminant levels for drinking water.

An inventory of existing and new wells and springs during this study provided additional information about the occurrence of groundwater on the western Hualapai Plateau. Many of the wells inventoried historically were no longer accessible because they have been destroyed or have collapsed at some point below the surface. Most wells only had one previous water level measurement, so no trends were apparent.

Data from 56 springs on and adjacent to the western Hualapai Plateau were compiled for this study, and new data were collected at 31 springs. Flow from the 31 springs measured for this study ranged from dry to about 345 gal/min. Eight springs were dry during at least one visit in 2018. Six springs were selected for repeat measurements to assess seasonal variations in flow. Temporal data from springs, where repeat measurements were available in the 1990s and during this study, indicate that spring flow was highly variable and likely related to seasonal and annual available precipitation that supports recharge. Access to springs from the most productive water-bearing zone, the Muav aquifer, presents significant challenges for development. Most of these springs are located in the bottom of tributary canyons to the Colorado River that are 1,500 ft or more below the elevation of the western Hualapai Plateau.

The high cost of exploration drilling to further explore the hydraulic properties of the Rampart Cave Member of the Muav Limestone on the Hualapai Plateau is prohibitive. Although a well intercepting a highly fractured zone within the Rampart Cave Member could hypothetically produce economic quantities of water, the findings of this study suggest that groundwater resources on the plateau cannot be deemed as a predictable source of water for economic development.

References Cited

Adams, D., and Comrie, A.C. 1997, The North American Monsoon: Bulletin of the American Meteorological Society, v. 78, p. 2197–2213.

Arizona Bureau of Geology and Mineral Technology, 1988, Geologic map of Santa Fe Railroad Company mineral holdings in northwestern Arizona: Arizona Bureau of Geology and Mineral Technology Miscellaneous Map MM-88A, scale 1:250,000.

Arizona Department of Water Resources, 2009, Arizona water atlas volume 4; Upper Colorado River Planning Area—Section 4.8, Peach Springs Basin: Arizona Department of Water Resources, p. 323–351.

Beard, L.S., and Lucchitta, I., 1993, Geologic map of the Valentine Southeast quadrangle, Mohave County, Arizona: U.S. Geological Survey Geologic Quadrangle Map 1711, scale 1:24,000, accessed January 17, 2020 at https://ngmdb.usgs.gov/Prodesc/proddesc_1216.htm.

Billingsley, G.H., Block, D.L., and Dyer, H.C., 2006, Geology of the Peach Springs 30' X 60' quadrangle, Mohave and Coconino Counties, northwestern Arizona: U.S. Geological Science Investigations Map 2900, 16 p., 1 plate, scale 1:100,000, available at https://pubs.usgs.gov/sim/2006/2900/.

Billingsley, G.H., and Wellmeyer, J.L., 2003, Geologic map of the Mount Trumbull 30' X 60' quadrangle, Mohave and Coconino Counties, northwestern Arizona: U.S. Geological Survey Geologic Investigations Series I-2766, scale 1:100,000, available at https://pubs.usgs.gov/imap/i2766/.

Billingsley, G.H., Wenrich, K.J., Huntoon, P.W., and Young, R.A., 1986, Breccia-pipe and geologic map of the southeastern Hualapai Indian Reservation and vicinity, Arizona: U.S. Geological Survey Open-File Report 86-458-B, scale 1:48,000, includes 26-p. pamphlet, available at https://doi.org/10.3133/ofr86458B.

Billingsley, G.H., Wenrich, K.J., Huntoon, P.W., and Young, R.A., 1999, Breccia-pipe and geologic map of the southwestern part of the Hualapai Indian Reservation and vicinity, Arizona: U.S. Geological Survey Miscellaneous Investigations Series Map I–2554, scale 1:48,000, 2 plates, 50 p., available at https://doi.org/10.3133/i2554.

Bills, D.J., Flynn, M.E., and Monroe, S.A., 2007, Hydrogeology of the Coconino Plateau and adjacent areas, Coconino and Yavapai Counties, Arizona: U.S. Geological Survey Scientific Investigations Report 2005–5222, 101 p., 4 plates, available at https://doi.org/10.3133/sir20055222.

Boyer, D.G., 1977, Water resources information survey for the Hualapai Indian Reservation, Arizona: Tucson, University of Arizona, Office of Arid Land Studies, Laboratory of Native Development, Systems Analysis and Applied Technology (NASDAT), 262 p.

Boyer, D.G., Ince, S., and Oben-Nyarko, K., 1978, Water resources development study for the Hualapai Indian Tribe: Tucson, University of Arizona, Office of Arid Land Studies, Laboratory of Native Development, Systems Analysis and Applied Technology (NASDAT), 76 p.

Cooley, M.E., 1976, Spring flow from pre-Pennsylvanian rocks in the southwestern part of the Navajo Indian Reservation, Arizona: U.S. Geological Survey Open-File Report 521–F, 15 p.

Darton, N.H., 1910, A reconnaissance of parts of northwestern New Mexico and northern Arizona: U.S. Geological Survey Bulletin 435, 88 p., available at https://pubs.usgs.gov/bul/0435/report.pdf.

Darton, N.H., 1915, Guidebook of the western United States—Part C, the Santa Fe Route: U.S. Geological Survey Bulletin 613, 194 p., available at https://pubs.er.usgs.gov/publication/b613.

Darton, N.H., 1925, A resume of Arizona geology: Arizona Bureau of Mines Bulletin 119, 298 p.

Devlin, N.J., 1976, Engineer's report on the possibilities of developing additional water supplies for the Hualapai Indian Tribe at Peach Springs, Arizona: N.J. Devlin, Consulting Engineer, Kingman, Arizona, July 27, 1976, 24 p.

Duffield, G.M., 2007, AQTESOLV for Windows Version 4.5 User's Guide: Reston, VA, HydroSOLVE, Incorporated, available at https://hwbdocuments.env.nm.gov/Los%20Alamos%20National%20Labs/General/37764.pdf.

Dutton, C.E., 1882a, The physical geology of the Grand Cañon district, *in* U.S. Geological and Geographical Survey Territory, Second Annual Report: Washington, Government Printing Office, p. 47–166.

Dutton, C.E., 1882b, Tertiary history of the Grand Cañon district: Tucson, University of Arizona Press, 264 p.

Farnsworth, R.K., Thompson, E.S., and Peck, E.L., 1982, Evaporation atlas for the contiguous 48 United States: National Oceanographic and Atmospheric Administration Technical Report National Weather Service Series 33, 26 p.

Flint, A.L., and Flint, L.E., 2007a, Application of the basin characterization model to estimate in-place recharge and runoff potential in the Basin and Range carbonate-rock aquifer system, White Pine County, Nevada, and adjacent areas in Nevada and Utah: U.S. Geological Survey Scientific Investigations Report 2007–5099, 20 p., available at https://pubs.usgs.gov/sir/2007/5099/.

Flint, L.E., and Flint, A.L., 2007b, Regional analysis of ground-water recharge, *in* Stonestrom, D.A., Constantz, J., Ferre, T.P.A, and Leake, S.A., eds., Ground-water recharge in the arid and semiarid southwestern United States: U.S. Geological Survey Professional Paper 1703, p. 29–60., available at https://pubs.usgs.gov/pp/pp1703/.

Freeze, A.R. and Cherry, J.A., 1979, Groundwater: Englewood Cliffs, New Jersey, Prentice-Hall, 604 p.

Hereford, R., Webb, R.H., and Grahm, S., 2002, Precipitation history of the Colorado Plateau Region, 1900 to 2000: U.S. Geological Fact Sheet 119–02, 4 p., accessed November 2015, at https://pubs.usgs.gov/fs/2002/fs119-02/

Hualapai Department of Natural Resources, 2010, Western Hualapai Plateau and Spencer creek watershed management—Special water study, Hualapai Reservation: Hualapai Department of Natural Resources, 52 p.

Hualapai Water Resources Program, 1999, Hualapai Reservation water quality assessment report 305(b): Prepared for the Hualapai Tribal Council by the Hualapai Water Resources Program with technical assistance from the U.S. Geological Survey, July 1999, 103 p.

Hualapai Water Resources Program, 2004, Hualapai Reservation water quality assessment report 305(b): Prepared for the Hualapai Tribal Council by the Hualapai Water Resources Program with technical assistance from the U.S. Geological Survey, July 2005, 223 p.

Hualapai Water Resources Program, 2009, Hualapai Reservation water quality assessment report 305(b): Prepared for the Hualapai Tribal Council by the Hualapai Water Resources Program with assistance from the U.S. Geological Survey, July 2009, 102 p.

Huntoon, P.W., 1977, Cambrian stratigraphic nomenclature and ground-water prospecting failures on the Hualapai Plateau, Arizona: Ground Water, v. 15, no. 6, p 426–433, https://doi.org/10.1111/j.1745-6584.1977.tb03190.x

Huntoon, P. W., 1978, Reply to the preceding Discussion by R. A. Young of "Cambrian Stratigraphic Nomenclature and Ground-Water Prospecting Failures on the Hualapai Plateau, Arizona:" Ground Water, v. 16, no. 4, 289–291, https://doi.org/10.1111/j.1745-6584.1978.tb03237.x

Knutson, C.L., Hayes, J.H., and Svoboda, M.D., 2007, Case study of tribal drought planning: The Hualapai Tribe, Natural Hazards Review, v 8, no 4, p. 125–131.

Koons, E.D., 1945, Geology of the Uinkaret Plateau, northern Arizona: Geological Society of America Bulletin, v. 56, no. 2, p. 151–180.

Koons, E.D., 1948a, Geology of the eastern Hualapai Reservation: Plateau, v. 20, no. 4, p. 53–60.

Koons, E.D., 1948b, High level gravels of western Grand Canyon: Science, v. 107, no. 2784, p. 475–476.

LANDFIRE, 2014, Existing Vegetation Type, LANDFIRE 1.4.0: U.S. Department of the Interior, U.S. Geological Survey, accessed 3 October 2019, at https://www.landfire.gov/viewer/viewer.html.

Lee, W.T., 1908, Geologic reconnaissance of a part of western Arizona: U.S. Geological Survey Bulletin 352, 107 p., available at https://pubs.usgs.gov/bul/0352/report.pdf.

Lucchitta, I., 1967, Cenozoic geology of the upper Lake Mead area adjacent to the Grand Wash Cliffs, Arizona: Unpublished Ph.D. dissertation, Pennsylvania State University, 218 p., 6 sheets, scales 1:31,680 and 1:63,360.

Macy, J.P., 2019, Controlled source audio-frequency magnetotellurics (CSAMT) data from the Grand Canyon West and Plain Tank Flat areas of the western Hualapai Reservation, Arizona: U.S. Geological Survey data release, https://doi.org/10.5066/P90KAJM4.

Maxey, G.B., and Eakin, T.E., 1949. Ground water in White River Valley, White Pine, Nye, and Lincoln Counties, Nevada: Nevada Department of Conservation and Natural Resources, Water Resources Bulletin 8, 59 p.

McKee, E.D., 1934, The Coconino Sandstone—Its history and origin, *in* Papers concerning the palaeontology of California, Arizona, and Idaho: Carnegie Institution of Washington, Publication 440, p. 77–135.

McKee, E.D., 1938, The environment and history of the Toroweap and Kaibab Formations of northern Arizona and southern Utah: Carnegie Institution of Washington, Publication 492, 268 p.

McKee, E.D., 1945, Stratigraphy and ecology of the Grand Canyon Cambrian, part 1, *in* McKee, E.D., and Resser, C.E., eds., Cambrian history of the Grand Canyon region: Carnegie Institution of Washington, Publication 563, p. 3–168.

Myers, S.M., 1987, Map showing groundwater conditions in the Peach Springs basin, Mohave, Coconino, and Yavapai Counties, Arizona—1987: Arizona Department of Water Resources Hydrologic Map Series Report 15, 1 plate, scale 1:125,000.

Natural Resources Consulting Engineers, 2011, Evaluation of the Peach Springs groundwater supply on the Hualapai Reservation: Prepared for the Hualapai Tribal Council by Natural Resources Consulting Engineers, Inc., 102 p.

Papadopulos, I.S. and H.H. Cooper, 1967. Drawdown in a well of large diameter, Water Resources Research, v. 3, no. 1, pp. 241–244.

PRISM Climate Group, 2020, PRISM climate data: Northwest Alliance for Computational Science and Engineering , Oregon State University, accessed January 29, 2020, at http://www.prism.oregonstate.edu/.

Reynolds, S.J., 1997, Geologic map of Arizona: Arizona Geological Survey Map M-35, 1 sheet, scale 1:1,000,000.

Richard, S.M., Reynolds, S.J., Spencer, J.E., and Pearthree, P.A., comps., 2000, Geologic map of Arizona: Arizona Geological Survey Map M-35, 1 sheet, scale 1:1,000,000.

Schrader, F.C., 1909, Mineral deposits or the Cerbat Range, Black Mountains, and the Grand Wash Cliffs, Mohave County, Arizona: U.S. Geological Survey Bulletin 397, 226 p., available at https://pubs.er.usgs.gov/publication/b397.

Sharma, P.V., 1997, Environmental and engineering geophysics: Cambridge, U.K., Cambridge University Press, 475 p.

Simpson, F., and Bahr, K., 2005, Practical magnetotellurics: Cambridge, U.K., Cambridge University Press, 254 p.

Stantec, 2009, Rehabilitation and Safe Yield Assessment, West Water Well, Hualapai Reservation, Arizona: Fresno, California, Stantec Consulting Corporation, 18 p.

Stewart, M.E., Taylor, W.J., Pearthree, P.A., Solomon, B.J., and Hurlow, H.A., 1997, Neotectonics, fault segmentation, and seismic hazards along the Hurricane fault in Utah and Arizona—An overview of environmental factors in an actively extending region in Mesozoic to recent geology of Utah: Geological Society of America Field Trip Guide Book, 1997 Annual Meeting, Salt Lake City, Utah, and Brigham Young University Geology Studies, v. 42, pt. 2, p. 235–254.

Tillman, F.D, Cordova, J.T., Leake, S.A., Thomas, B.E., and Callegary, J.B., 2011, Water availability and use pilot; methods development for a regional assessment of groundwater availability, southwest alluvial basins, Arizona: U.S. Geological Survey Scientific Investigations Report 2011–5071, 118 p., available at https://pubs.usgs.gov/sir/2011/5071/.

Trapp, R.A., and Reynolds, S.J., 1995, Map showing names and outlines of physiographic areas in Arizona used by the Arizona Geological Survey with base map showing township and range only: Arizona Geological Survey Open File Report, OFR-95-2b, 1 map sheet, scale 1:1,000,000.

Twenter, F.R., 1962, Geology and promising areas of groundwater development in the Hualapai Reservation, Arizona: U.S. Geological Water-Supply Paper 1576–A, 1 plate, 38 p.

U.S. Environmental Protection Agency, 2003, Current drinking water standards, national primary and secondary drinking water regulations: Washington, D.C., U.S. Environmental Protection Agency, accessed May 14, 2019, at http://www.epa.gov/safewater/mcl.html.

U.S. Geological Survey, 2019, National Water Information System—Web interface, accessed November 22, 2019, at http://dx.doi.org/10.5066/F7P55KJN.

U.S. Geological Survey, variously dated, National field manual for the collection of water-quality data: U.S. Geological Survey Techniques of Water-Resources Investigations, book 9, chaps. A1–A10, available at http://pubs.water.usgs.gov/twri9A.

Wenrich, K.J., Billingsley, G.H., and Huntoon, P.W., 1996, Breccia-pipe and geologic map of the northwestern part of the Hualapai Indian Reservation and vicinity, Arizona: U.S. Geological Survey Geologic Investigations Map I–2522, 2 pls., scale 1:48,000, 16 p., available at https://doi.org/10.3133/i2522.

Wenrich, K.J., Billingsley, G.H., and Huntoon, P.W., 1997, Breccia-pipe and geologic map of the northeastern part of the Hualapai Indian Reservation and vicinity, Arizona: U.S. Geological Survey Miscellaneous Investigations Series I–2440, scale 1:48,000, 19 p., available at https://doi.org/10.3133/i2440.

Wilson, E.D., and Moore, R.T., 1959, Geologic map of Mohave County, Arizona: Prepared by the Arizona Bureau of Mines and University of Arizona, Tucson, 1 plate, scale 1:375,000.

Young, R.A., 1966, Cenozoic geology along the edge of the Colorado Plateau in northwestern Arizona: St. Louis, Washington University, Ph.D. dissertation, 4 plates, 167 p.

Young, R. A.,1978, Discussion of "Cambrian stratigraphic nomenclature and ground-water prospecting failures on the Hualapai Plateau, Arizona": Ground Water, v.16, no. 4, p. 287–289. https://doi.org/https://doi.org/10.1111/j.1745-6584.1978.tb03236.x.

Young, R.A., 1987, Colorado Plateau, landscape development during the Tertiary, *in* Graf, W.L., ed., Geomorphic systems of North America: Geological Society of America Centennial, Special Volume 2, p. 266–276.

Young, R.A., 1999, Nomenclature and ages of Late Cretaceous(?)—Tertiary strata in the Hualapai Plateau region, northwest Arizona, *in* Billingsley, G.H., Wenrich, K.J., Huntoon, P.W., and Young, R.A., Breccia-pipe and geologic map of the southwestern part of the Hualapai Indian Reservation and vicinity, Arizona: U.S. Geological Survey Miscellaneous Investigations Series Map I–2554, 2 plates, scale 1:48,000, appendix, p. 21–50.

Young, R.A., 2007, The geology and hydrology of Tertiary groundwater aquifers and the impact of shallow rock quarrying in upper Milkweed Canyon: Special Report to the Cultural Resources Department, Hualapai Tribe, 25 p.

Zonge, K., 1992, Broadband electromagnetic systems, *in* Van Blaricom, R., ed., Practical geophysics II for the exploration geologist: Northwest Mining Association, 96 p.

Appendixes

Appendix 1 and 2 contain tabulated data that describe the well cutting, pump test, water-quality, and well and spring inventory data. These data are compiled into five separate comma-delineated tables that can be found online at https://doi.org/10.3133/sir20205025 and https://doi.org/10.5066/P90KAJM4

Menlo Park Publishing Service Center, California
Manuscript approved for publication March 11, 2020
Edited by Phil A. Frederick
Layout and design by Kimber Petersen
Illustration support by JoJo Mangano

ISSN 2328-0328 (online)